Unconventional superconductivity in Sr_2RuO_4

Ying Liu[1,2,3] and Zhi-Qiang Mao[4]

[1]Department of Physics and Materials Research Institute, Pennsylvania State University, University Park, PA 16802, U.S.A.

[2]Key Laboratory of Artificial Structures and Quantum Control (Ministry of Education), Department of Physics and Astronomy, Shanghai Jiao Tong University, Shanghai 200240, China

[3]Collaborative Innovation Center of Advanced Microstructures, Nanjing 210093, China.

[4]Department of Physics and Engineering Physics, Tulane University, New Orleans, LA 70118, U.S.A.

Abstract

Sr_2RuO_4, featuring a layered perovskite crystalline and quasi-two-dimensional electronic structure, was first synthesized in 1957. Unconventional, *p*-wave pairing was predicted for Sr_2RuO_4 by Rice and Sigrist and Baskaran shortly after superconductivity in this material was discovered in 1994. Experimental evidence for unconventional superconductivity in Sr_2RuO_4 has obtained in the past two decades and reviewed previously. In this article, we will first discuss constraints on the pairing symmetry and the mechanism of superconductivity in Sr_2RuO_4 and summarise experimental evidence supporting the unconventional pairing symmetry accumulated to date. We will then present several aspects of the experimental determination of the unconventional superconductivity in Sr_2RuO_4 in some detail. In particular, we will discuss the phase-senistive measurements that have played an important role in the determination of the pairing symmetry in Sr_2RuO_4. The responses of superconductivity to the mechanical perturbations and their implications on the mechanism of superconductivity are discussed. A brief survey of various non-bulk Sr_2RuO_4 is also included to illustrate the many unusual features resulted from the unconventional nature of superconductivity in this material system. Finally, we will discuss some outstanding unresolved issues on Sr_2RuO_4 and provide an outlook of the future work on Sr_2RuO_4.

Key wards: Unconventional superconductivity, strongly correlated electrons

1. Introduction

The Bardeen-Cooper-Schrieffer (BCS) theory[1] of superconductivity shows that the origin of superconductivity is the formation and condensation of Cooper pairs in momentum space. In this theory, the symmetry property of the wave function of the electron pairs in the BCS theory, known as an *s*-wave pairing state, a is a constant in the momentum space. The interaction responsible for the pairing in the BCS theory is the electron-phonon interaction. Superconductors lacking either of these two essential features are considered in general unconventional superconductors, a definition adopted here. Shortly after the discovery of the BCS theory, it was realized that superconducting states more complex than that discussed in the BCS theory are also possible.

In a many-electron system with translational invariance, interchanging two electrons is equivalent to inverting their relative coordinates. Therefore, symmetry requirements from interchanging two identical particles are equivalent to those of inversion. For a superconductor with an inversion symmetry, only an even-parity, spin-singlet, or odd-parity, spin-triplet pairing is allowed. A mixed pairing state is possible if the inversion symmetry is absent, as in the case of an interface system between two dissimilar materials[2] or a non-centrosymmetric material[3]. In a single crystalline superconductor, the symmetry property of the pairing state is usually denoted as a function of the wave vector, $\boldsymbol{k} = (k_x, k_y, k_z)$, where *x*, *y*,

z are real-space Cartesian coordinates. The superconducting order parameter of both spin-singlet and spin-triplet superconductor can be expressed in the tensor form[4], $\Delta = -i\sigma_y d_0$ for spin-singlet and $\Delta = -i\sigma_y(\boldsymbol{d}\cdot\boldsymbol{\sigma})$ for spin-triplet superconductors, where $i = \sqrt{-1}$, d_0 is a scalar, $\boldsymbol{d} = (d_x, d_y, d_z)$ is a vector and $\boldsymbol{\sigma} = (\sigma_x, \sigma_y, \sigma_z)$ are the Pauli matrices. For spin-singlet superconductors, only a single component is needed to represent the superconducting order parameter (the wave function of the Cooper pair). For spin-triplet superconductors, however, each of the three spin channels is represented by its own wave function. Under the rotation of the spatial coordinates, $\boldsymbol{d} = (d_x, d_y, d_z)$ follows the same transformation as that of any other vectors and therefore is referred to as the d-vector. The amplitude of the d-vector is the order parameter while its direction is the norm of the plane to which the projection of the total spin of any Cooper pair is zero, meaning that electrons in a spin-triplet superconductor form an equal spin pairing state in this plane.

Pairing states allowed by symmetry considerations can be realized only if the required attractive interaction or interactions are available in a particular channel or channels. In the presence of a rotational symmetry, the interaction potential can be decomposed into channels with different orbital angular momenta, l. The superconducting energy gap in l channel, Δ_l, is given by $\Delta_l = 2\varepsilon_l \exp(-2/N_0 V_l)$, where ε_l is a characteristic energy, N_0 is the density of states at the Fermi energy, and V_l is interaction in the l channel. States with $l = 0, 2$ ... correspond to s-, d-wave ... (even-parity) and those of $l = 1, 3$ ... to p-, f-wave ... (odd-parity) pairing states. Electrons usually pair in the channel of the largest V_l, corresponding to the highest T_c, to attain the largest condensation energy, even though other V_l's may also be attractive and substantial.

The synthesis of Sr_2RuO_4 was first reported in 1959[5]. Sr_2RuO_4 entered contemporary condensed matter physics as a substrate material for high-T_c superconductors[6] and as a possible 4d transition metal oxide counterpart of the 3d high-T_c cuprates in the search of new superconductors [7] before superconductivity was discovered in 1994[8]. The discovery generated much interest because Sr_2RuO_4 was (and still is) the only transition metal oxide with a layered perovskite crystalline structure that becomes superconducting without the presence of Cu. In fact, Sr_2RuO_4 is the only known superconducting ruthenium oxide under ambient pressure. The study of Sr_2RuO_4 was therefore believed to be useful for understanding high-T_c superconductivity in cuprates. However, Rice and Sigrist[9] realized that Sr_2RuO_4 is closer to ^{3}He than to high-T_c cuprates. They also noticed that the insulating solid-solution of $Sr_2Ir_{1-x}Ru_xO_4$ features an $S = 1$ correlation before an insulator-to-metal transition takes place (as an increasing x) at a critical point of x = 0.2, and predicted p-wave pairing in Sr_2RuO_4. Baskaran[10] also predicted spin-triplet, p-wave pairing in Sr_2RuO_4, relying on the experiment showing that $Sr_2Ir_{1-x}Ru_xO_4$ features an $S = 1$ correlation, and the assumption that Hund's rule coupling may be at work in Sr_2RuO_4. These theoretical predictions motivated a series of experiments that provided strong support to the predicted unconventional pairing state in this material.

So far, several reviews on Sr_2RuO_4 have already been published. Mackenzie and Maeno reviewed the majority of the results available in literature up to 2003[11], followed by a more recent update in 2012 by Maeno and co-workers[12]. Other reviews[13,14,15,16,17] were also published over the years - we apologize if we have missed any – amost all of which heavily emphasize the experimental side of the literature. Following this trend, the present authors will skip most theoretical work done so far on Sr_2RuO_4. In particular, we will not review the large body of theoretical work on the mechanism of superconductivity in Sr_2RuO_4, including the effort trying to identify the interaction responsible for the pair formation because this issue is much less clear than the pairing symmetry at the time of writing. Even within this rather restricted scope, we will not be able to cover all relevant papers published on Sr_2RuO_4. The unfortunate ommisions are due to time limit rather than judgement on the value of the missed papers.

We will specifically focus on experimental work on Sr_2RuO_4 that we feel has not been covered in sufficient detail or not at all in the previous reviews. We also include discussion on some of the most recent developments in the field and provide a short list of unresolve issues as well as an outlook of the future directions in Sr_2RuO_4 research.

2. Constraints on the pairing symmetry and mechanism of superconductivity in Sr_2RuO_4

The structual and electronic properties of Sr_2RuO_4 provide constraints on the pairing symmetry of this superconductor. Sr_2RuO_4 has a K_2NiF_4 structure, a layered perovskite with $a = b = 3.87$ Å and $c = 12.74$ Å. Its crystalline symmetry is characterized by a D_{4h} space group, featuring four-fold rotational and inversion symmetries. Therefore the pairing symmetry in Sr_2RuO_4 must be purely spin-triplet if it is spin-triplet as suggested by the available experiments. No mixed pairing state is allowed, at least in the bulk. This constraint is not applicable to pairing state on the surface of the material. On the other hand, on the *ab* surface of a Sr_2RuO_4 crystal cleaved in a reasonably high temperature, the octahedral of RuO_6 were found to rotate for a small angle[18], which likely makes the room-temperature cleaved *ab* surface not superconducting at all because of the structural distortion[19].

The electronic band structure of Sr_2RuO_4 near the Fermi energy is dominated by t_{2g} orbitals of Ru^{4+}, d_{xz}, d_{yz}, and d_{xy}. Within the tight binding approximation, d_{xz} and d_{yz} hibridize to form two one-dimensional (1D) bands and d_{xy} orbitals result in a two-dimensional (2D) band[20,21]. The Fermi surface of Sr_2RuO_4 consists three sheets, denoted as α, β, and γ, with α and β formed primarily by the 1D bands and γ essentially the 2D band. In addition, β, and γ sheets are electron-like, but the α sheet is the hole-like. Results from quantum oscillation [22] and angle-resolved photo emission spectroscopy (ARPES) experiments[23] are consistent with the band structure calculations. The three-sheet Fermi surface for Sr_2RuO_4 was found to be rather cylindrical with little k_z dependence, suggesting that Sr_2RuO_4 is quasi 2D electronically as well. The 2D nature of normal-state electronic properties of Sr_2RuO_4 makes it highly likely that superconductivity in Sr_2RuO_4 is two-dimensional (2D) in nature, with no k_z dependence in the superconducting order parameter. On the other hand, a hydrostatic pressure study[24], to be discussed in more detail below, revealed that Sr_2RuO_4 becomes increasingly 2D electronically while the T_c value drops at the same time, which seems to suggest that the superconducting order parameter may have k_z dependence, as suggested previously[25].

Within the odd-parity, spin-triplet scenario, five possible spin-triplet pairing states are allowed in 2D in the tetragonal symmetry point group. The spin-orbit coupling of 4d electrons/holes is in general of considerable strngth. Indeed, a comparison between the electronic band structure obtained from calculation taking into account the spin-orbit coupling and those obtained in the AREPES measurements indicate that the spin-orbit coupling energy in Sr_2RuO_4 can be as high as 90 meV[26]. The symmetry properties of the superconducting order parameter of these five odd-parity pairing states in strong spin-orbit coupling limit is listed in Table 1[9]. The representations in the weak spin-coupling limit are found in the literature. Among these five pairing states in the strong spin-orbit coupling limit, four of them (Γ^-_{1-4}) are one-component representations with the d-vector in the *ab* plane while the fifth, the Γ^-_5 state, is a two-component representation with the d-vector along the *c* axis, featuring a doubly degenerate, time reversal symmetry breaking state (known as the $k_x \pm i\, k_y$ state).

Table 1. Rice-Sigrist proposal[9] on spin-triplet pairing states in Sr_2RuO_4 with a point group D_{4h}.

Pairing state	J, J_z	$\boldsymbol{d}(\boldsymbol{k})$	Analog in ^{3}He
A_{1u} (Γ^-_1)	0, 0	$\boldsymbol{x}\, k_x + \boldsymbol{y}\, k_y$	B-phase
A_{2u}(Γ^-_2)	1, 0	$\boldsymbol{x}\, k_y - \boldsymbol{y}\, k_x$	B-phase
B_{1u}(Γ^-_3)	2, ±2	$\boldsymbol{x}\, k_x - \boldsymbol{y}\, k_y$	B-phase
B_{2u}(Γ^-_4)	2, ±2	$\boldsymbol{x}\, k_y + \boldsymbol{y}\, k_x$	B-phase
E_u(Γ^-_5)	1, ±2	$\boldsymbol{z}\, (k_x \pm i\, k_y)$	A-state

The relevant interactions enabling unconventional pairing in Sr_2RuO_4, the mechanism of superconductivity, must rely on the magnetic and electrical properties of the normal state, as shown by the realization of the spin-triplet pairing in superfluid ^3He[27]. For conventional superconductors, the electron-phone interaction as the source of interaction for the *s*-wave pairing that was put forward in the BCS theory was inspired by the observation of isotope effect and established to a large extent by a careful analysis of single-particle tunneling spectra to energies much higher than the superconducting energy gap. Similar results are not available for Sr_2RuO_4. In fact, results from the isotope effect experiment on Sr_2RuO_4[28] are inconclusive. Therefore, the constraint on the mechanism of superconductivity in Sr_2RuO_4, including the responses of the T_c to the mechanical perturbation, such as hydrostatic pressure and uniaxial stresses/strains to be discussed below, is relatively weak. Therefore our discussion on the mechanism of superconductivity in Sr_2RuO_4 will be brief.

3. Summary of experimental evidence for unconventional superconductivity in Sr_2RuO_4

Experimental evidence for unconventional superconductivity in Sr_2RuO_4 includes the observation of following phenomena: 1) Power-law behavior in various thermodynamic, magnetic, transport, and ultrosound properties even at a temperature much lower than T_c [29,30,31,32,33], which suggests the presence of a large number of quasiparticles and therefore nodes in the order parameter or band-dependent superconducting energy gaps found in multiband superconductivity; 2) the absence of Hebel-Slichter coherence peak NMR and NQR $1/T_1$ measurements[34]; 3) the non-monotonic temperature dependence in the critical current of Pb-Sr_2RuO_4-Pb junctions[35]; (observations of 3) and 4) suggest that the pairing symmetry in Sr_2RuO_4 is different from that of the conventional *s*-wave); 5) the extremely sensitivity the occurrence of superconductivity in Sr_2RuO_4 was found to be to the presence of impurities[36], a characteristic of a non-*s*-wave that requires the electron mean-free-path in the normal state to be larger than zero-temperature coherence length, which is large for Sr_2RuO_4 because of its low T_c value; 6) a square vortex lattice featuring unconventional parameters[37], 7) zero-bias conductance peak found in tunneling measurements suggesting the existence of Andreev surface bound states resulting from the change of internal phase of the superconducting order parameter[38,39]. All these measurements suggest that Sr_2RuO_4 is an unconventional, non-*s*-wave superconductor.

First direct experimental evidence for the spin-triplet pairing in Sr_2RuO_4 came from NMR Knight shift[40] with the magnetic field applied along the *ab* plane. The spin susceptibility was found to be unchanged as the temperature was lowered to below the T_c in Sr_2RuO_4, which is marked different from that expected from a spin-singlet superconductor but consistent with that of a spin-triplet superconductor with its d-vector aligned along the *c* axis. The result of the NMR Knight shift measurements was confirmed by polarized-neutron scattering measurements[41]. An important issue in the analysis of the Knight shift data is the orbital spin susceptability, which usually relies on the so-called K-χ (Knight shift *vs*. bulk susceptibility) plot. Recently, Knight shifts of both the Ru and Sr site in the Sr_2RuO_4 were performed out. Subtracting Knight shift at Sr site from that of the Ru site seems to have circumvented this issue, indicating that the original analysis is valid. Subsequent NMR Knight shift measurements with the magnetic field aligned along the *c* axis[42,43], which was difficult to carry out because the very low value of upper critical field, did not reveal the drop expected assuming that the d-vector is along the *c* axis. This observation suggests that the nature of superconductivity is more complex. It was suggested that even though the d-vector is aligned along the c axis in the zero and very low magnetic fields, it might be rotated with the application of a *c*-axis field in a a-axis field of 400 G or even lower so that the Knight shift will remain unchanged across T_c. This assumption, however, needs to be recocnciled with theoretical consideration and experimental data suggesting that spin-orbit coupling in Sr_2RuO_4 is actually strong.

Given the unresolved issue in the interpretation of the Knight shift result, independent determination on the parity of the orbital part of the Cooper pair wave function is important. Within the spin-triplet scenario, the direction and the parity of the d-vector can be determined by Josephson effect based experiments. In this regard, the Josephson coupling between an *s*-wave superconductor and

Sr_2RuO_4 was found to be zero along the *c* axis and non-zero in the in-plane direction[44] - a selection rule consistent with a d-vector being locked to the *c* axis. Within the five possible states listed in Table 1, the Γ^-_5 is the only state with a *c*-axis oriented d-vector. Superconducting quantum interference device (SQUID) based phase sensitive measurements[45], discussed in more detail below, showed that the phase of the superconducting order parameter changes by π under a 180-degree rotation, providing direct evidence for the orbital part of the wave function of the Cooper pairs in Sr_2RuO_4 being of an odd parity.

Within the Γ^-_5 picture, however, only a single chiral domain, $k_x + i\,k_y$ or $k_x - i\,k_y$, was present in Sr_2RuO_4 crystals during the phase-sensitive measurement, which were as large as a minimeter. Another consequence of the the pairing state in Sr_2RuO_4 being that of the Γ^-_5 is that the $k_x + i\,k_y$ and $k_x - i\,k_y$ domains separated by domain wall should be found under certain conditions. So should be chiral surface currents. Indeed, a spontaneous magnetic field was detected in Sr_2RuO_4 by μSR[46] and polar Kerr rotation[47], showing that Sr_2RuO_4 is a time-reversal symmetry-breaking superconductor, consistent with that expected for Γ^-_5 state. On the other hand, even though a Josephson effect study did reveal that an interference pattern asymmetric with respect to the reversal of the magnetic field applied along the junction plane[48], which is consistent with existence of $k_x + i\,k_y$ or $k_x - i\,k_y$ domains in Sr_2RuO_4, low-temperature scaning SQUID microscopy[49,50] and phase-sensitive measurements[51] on the chiral surface currents only turned out an upper limit that is two or three orders of magnitude smaller than that predicted by Bogoliubov-de Gennes calculations[52]. These inconsistencies are unsettling as the argument/evidence leading to Sr_2RuO_4 being in Γ^-_5 state seems to be quite strong.

3. Phase-sensitive determination of the pairing symmetry

3.1. Josephson coupling between a spin-singlet and spin-triplet superconductor: Theory

Josephson coupling between two superconductors can be understood as a result of the overlap between the superconducting order parameters of the two adjacent superconductors, or, alternatively, the tunneling of the Cooper pairs from one superconductor to the other. Without spin-orbit coupling, spin is a good quantum number. This would in turn make the spin-singlet and spin-triplet wave function orthogonal, resulting in a zero overlap of the wave function and consequently the absence of Josephson coupling. For a Josephson tunnel junction between an *s*- and a *p*-wave superconductor, the Josephson coupling is facilitated by spin-orbit coupling[53,54,55]. However, it was pointed out that complications are present in the case of a weak link where Josephson coupling between an *s*- and a *p*-wave superconductor may still be present even when spin-orbit coupling is zero[56]. Using a tunneling Hamiltonian formulism, the supercurrent current in a Josephson junction between a spin-singlet and spin-triplet superconductor is of the form

$$I(\varphi) = 2e\,\mathrm{Im}\int \lambda T^2 F^* K(x)\left(\left[\vec{d}(\vec{k},\vec{x})\cdot(\vec{k}\times\vec{n})\right]\right)d\vec{x}d\vec{k} \qquad (1)$$

where λ is a dimensionless parameter of order of unity representing the spin-orbit part of the tunneling matrix T, F* is the Gor'kov function in the spin-singlet superconductor, K(x) is the kernel linking the Gor'kov function with the order parameter in the spin-triplet function. A similar expression based on a semiclassical theory with the form

$$j_s = N(E_F^S)v_F^S\int\frac{d\Omega^S}{4\pi}(\hat{x}\cdot\hat{p})T\sum\pi\frac{\mathrm{Re}(c_{21}s_{21}^*)\mathrm{Im}\left[\Psi^*\vec{d}\cdot(\vec{n}\times\vec{p}_{//})\right]}{(\varepsilon_n^2+|\Psi|^2)^{1/2}(\varepsilon_n^2+|d|^2)^{1/2}} \qquad (2)$$

was obtained, where c_{21} and s_{21} are the spin-orbit and spin-independent parts of the transmission matrix that connects the incoming and outgoing waves at the interface, Ψ is the order parameter of the singlet superconductor, $\boldsymbol{d}(\boldsymbol{k})$ is the order parameter for the spin triplet, $\boldsymbol{k}$ is the wave vector, $\boldsymbol{n}$ is the normal vector for the interface, $p_{//}$ is the component of momentum in the direction perpendicular to $\boldsymbol{n}$, and $\varepsilon_n = (2n+1)\pi T$ is the Matsubara frequencies. It is seen that no term similar to $\mathrm{Re}(c_{21}s_{21}^*)$ was included

explicitly in Eq. 1. Since $\boldsymbol{d}(\boldsymbol{k})$ is related to spins and $\boldsymbol{k} \times \boldsymbol{n}$ is essentially the angular momentum, Eqs. 1 and 2 reflect the physics that it is the spin-orbit coupling, which makes spin not a good quantum number, that is responsible for the conversion between spin-singlet and spin-triplet Cooper pairs. Essentially, for a planar tunnel junction with translational invariance along the junction plane, Eqs. (1) and (2) suggest that the Josephson current density is of the form

$$J_s \sim <\Psi_s \boldsymbol{d}(\boldsymbol{k}) \bullet (\boldsymbol{k} \times \boldsymbol{n})>_{FS} \qquad (3)$$

where Ψ_s and $\boldsymbol{d}(\boldsymbol{k})$ are order parameters for *s*- and *p*-wave superconductors, respectively, as stated above, and $<\ldots>_{FS}$ denotes an appropriate average over the Fermi surface.

The Josephson current between Sr_2RuO_4 and an *s*-wave superconductor will then depend on three factors: 1) The difference in the overall phase of the superconducting order parameter of the two superconductors. This relative phase is the only factor that determines the supercurrent for conventional Josephson junctions; 2) The orientation of the d-vector with respect to the crystalline axes and the junction interface. If the d-vector in Sr_2RuO_4 is indeed along the *c* axis, non-zero supercurrent current is expected along the in-plane direction, but not along the *c* axis for or a Josephson junction between Sr_2RuO_4 and an *s*-wave superconductor[44]; 3) The relative phase of the spin-orbit transmission amplitude c_{21} and the spin-independent amplitude s_{21}. This relative phase will in principle depend on details of the junction. However, it was suggested that for certain materials combination, this relative phase could depend on materials only. In any case, the sign of the Josephson coupling in the two junctions shown in Fig. 2, with an **n** and a –**n** respectively, is opposite to one another, making it a dc SQUID consisting of a 0- and π-junction.

3.2. Josephson coupling between an s-wave superconductor and Sr_2RuO_4

According to Eqs. 1 and 2, Josephson coupling between an *s*- and a *p*-wave superconductor through a planar tunnel junction is zero along the direction of the *d*-vector. Experimentally the Josephson coupling between an *s*-wave superconductor In and Sr_2RuO_4 was measured in *c*-axis and in-plane junctions prepared by pressing freshly cut pure In wire directly onto a cleaved *ab* or polished *ac* face of Sr_2RuO_4[44]. Pressed In junctions prepared on cleaved *ab* face were found to show no finite critical current, even though good contact between In and Sr_2RuO_4 was evidenced by the observation of an excessive current, or zero-biased conductance peak (ZBCP), suggesting that the absence of the Josephson coupling between In and Sr_2RuO_4 along the *c* axis is not due to junction quality. This is relevant as it is known that superconductivity is suppressed on the *ab* face by the rotation of RuO_6 octehedral[18]. However, estimates on the relevant characteristic lengths, the normal coherence length and the depth of the non-superconducting surface on Sr_2RuO_4 make it unlikely that absence of Josephson coupling between an *s*-wave superconductor and Sr_2RuO_4 along the *c* axis is not due to the intrinsic reason. Josephson coupling between In and Sr_2RuO_4 was detected along the in-plane direction, even though the disorder on the mechanically polished *ac* face of the crystal is clearly stronger than that of the cleaved *ab* face, consistent with the theoretical expectation based on Eq. 1 and that the d-vector in Sr_2RuO_4 is long the *c* axis. Thus this selection rule suggests that the *d*-vector is along the *c* axis, which is the Γ_5^- state within Rice-Sigrist scheme (Table 1) in the spin-triplet pairing picture.

On the quantitative level, however, two issues are yet to be resolved. First, the temperature dependence of the critical current density needs to be clarified. Theory predicts that the critical current should follow the behavior, $I_c \sim (T_c - T)^{n/2}$, where *n* is determined by pairing symmetry, which should be 1 for a Josephson junction between an *s*- and a *p*-wave superconductor[56]. Experimentally, the temperature dependence of the critical current in a Josephson junction is linear, as shown in Fig. 1B. Interestingly, the same linear temperature dependence was also seen in Josephson junctions of high-T_c cuprates featuring an unconventional, d-wave pairing symmetry[57]. It was argued that experimental issues, mostly those associated with sample homogeneity, may be the dominant factor determining the temperature dependence of the critical current in those high-T_c junctions. Similarly, the observed temperature

dependence of Josepson current of an In/Sr_2RuO_4 might be unrelated to the pairing symmetry of Sr_2RuO_4; Second, the strength of the coupling measured by the critical current, I_c, appears to be larger than that expected in theory. For two dissimilar *s*-wave superconductors, the Josephson coupling at $T = 0$ is given by the Ambegaokar-Baratoff (A-B) formula[58], which states that I_cR_N , where R_N is the junction resistance in the normal state, is a universal value determined by the energy gaps of the two superconducting electrodes, independent of the details of the junction, reflecting that fact that both quasiparticle and Cooper pair tunnelings are subjecting to the same tunneling matrix. Experimentally, the A-B limit was found to be a good measure of the upper limit of the Josephson coupling if the bulk gap values are used, likely due to that fact that the superconducting energy gaps are suppressed at the junction interface, causing the I_c to fall below its maximum value. To estimate the size of Josephson coupling strength between an *s*-wave superconductor and Sr_2RuO_4, the value for the energy gap in the bulk can be estimated from T_c using the BCS result, $\Delta = 1.76k_BT_c$, an A-B limit of 0.5 mV is obtained for In/Sr_2RuO_4 junction. At $T = 0.3$ K, values of I_cR_N were found to be as high as 0.10 mV for In/Sr_2RuO_4 samples (Fig. 1B), a substantial fraction of the A-B limit. This value is surprising as the Josephson coupling between an *s*- and a *p*-wave superconductor should be small based on Eqs 1 and 2. Indeed, theoretical calculations that yielded an I_cR_N value for *s*- and *p*-wave Josephson junction two or three orders of magnitude smaller than the A-B limit[56,59], an issue to be resolved.

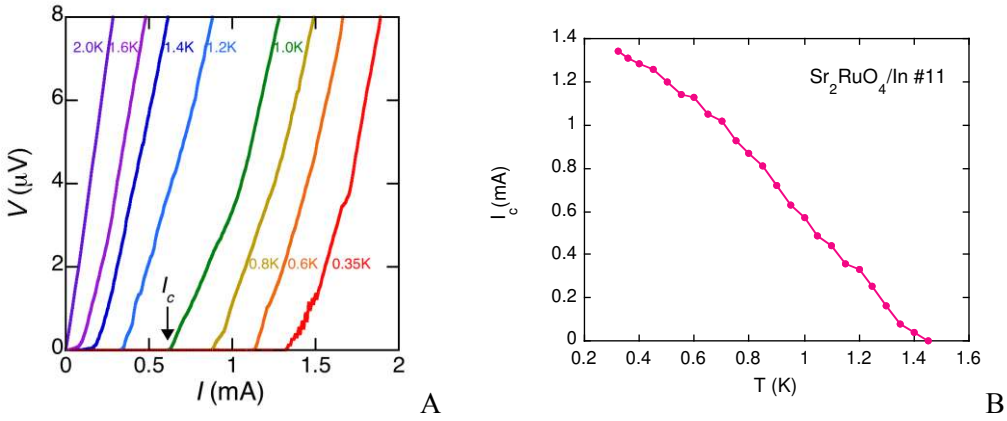

Figure 1. a) Current (I) - voltage (V) curves of an in-plane In/Sr_2RuO_4 junction. The critical current (I_c) is defined by the onset of a finite voltage; b) The critical current (I_c) *vs* temperature (T) for an in-plane junction ($R_N = 0.08\Omega$). Taken from Refs. 44 and 16.

3.3. SQUID-based phase-sensitive experiments on bulk Sr_2RuO_4

It is widely believe that the *d*-wave pairing symmetry in high-T_c cuprates was settled by SQUID[60] or tricrystal[61] based phase-sensitive measurements. These measurements help determine the directional dependence of the phase of the superconducting order parameter that can not be interpreted other than a d-wave pairing symmetry. Similarly, the unambiguous determination of the directional dependence of the order parameter for Sr_2RuO_4 also requires phase-sensitive measurements, due originally to Geshkenbein, Larkin, and Barone (GLB)[62], proposed for heavy fermion superconductors. The idea was re-discovered in the context of high-T_c superconductors[63]. The approach to phase-sensitive measurements carried out by the authors is illustrated in Fig. 2. Essentially we build a phase-sensitive toolkit that includes the same-side, the corner, and the opposite-side SQUID structures. The latter is that proposed originally by GLB. According to Eq. 3, the Josephson currents in a SQUID with its two Josephson junctions prepared on the opposite faces of a spin-triplet superconductor (the two junctions have a normal vector in $\boldsymbol{n}$ and $-\boldsymbol{n}$, respectively) are out of phase with one another by 180 degrees, making the SQUID a π-SQUID similar to those found in a ferromagnetic SQUID[64], yielding a minimum in the quantum interference pattern of $I_c(\Phi)$, where Φ is the total amount of the flux threaded in the SQUID loop, as opposed to a maximum if Sr_2RuO_4 were an *s*- or *d*-wave superconductor. Except the opposite-side GLB SQUID, the same-side and

the corner Josephson junctions were also fabricated and measured as references, with the results compared againt their respective expected behaviors[16].

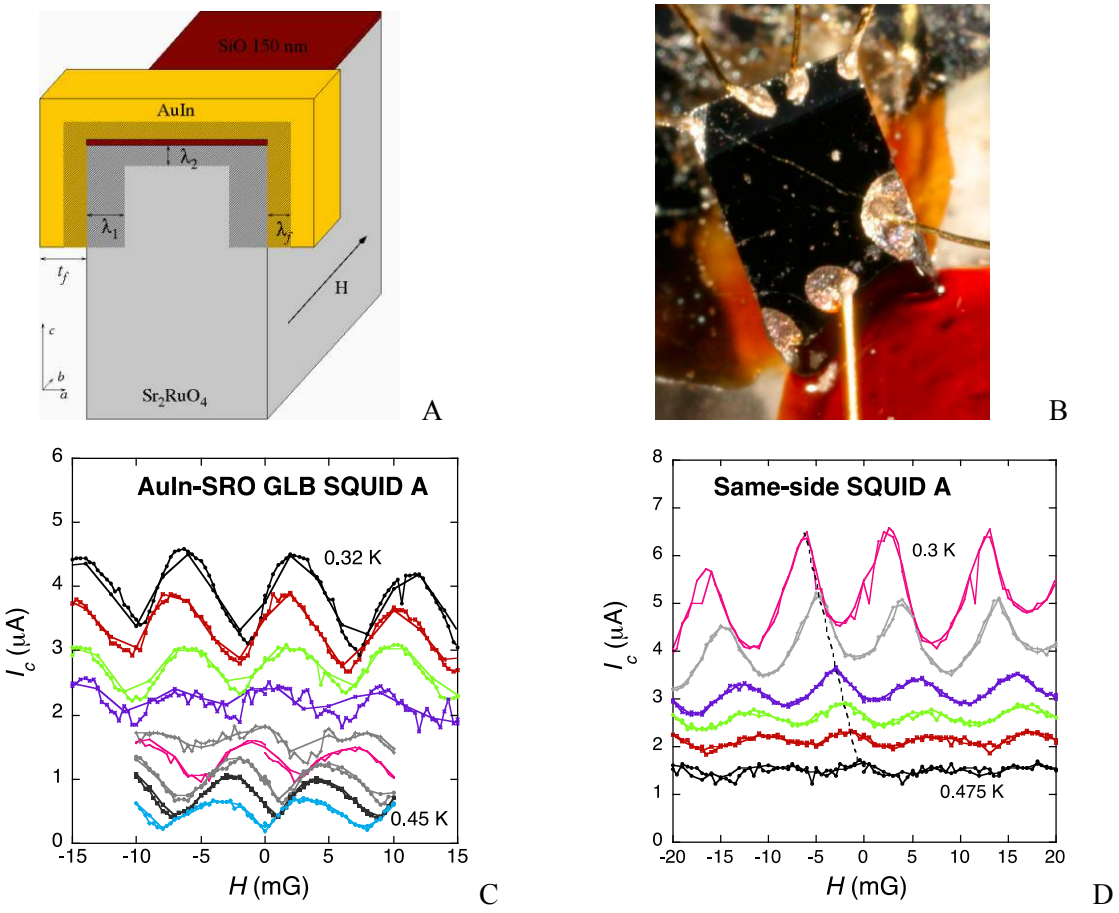

Figure 2. A) Schematic of a GLB $Au_{0.5}In_{0.5}$-Sr_2RuO_4 SQUID. The two Josephson junctions are on the left and the right sides of the crystal; B) Obtical picture of a real device. The Au wires are 50 μm in diameter. The top face of the crystal is the cleaved ab face, and is roughly 1 mm in width; C) $I_c(H)$ for a AuIn-Sr_2RuO_4 SQUID prepared on the opposite sides; D) and the same side of a Sr_2RuO_4 crystal. Taken from Refs. 16 and 45.

Because of the sensitivity of superconductivity in this material to disorder, superconducting thin films are difficult to prepare (see below for more details), making tricrystal-type phase-sensitive measurements not possible. SQUID based phase-sensitive measurements on Sr_2RuO_4 require the preparation of SQUIDs involving an *s*-wave superconductor and Sr_2RuO_4 using single crystals. To prepare single-crystal based Josephson junctions, such as a GLB SQUID shown in Fig. 2A, *ac* faces of a Sr_2RuO_4 crystal need to be prepared by mechanical polishing. Thermally evaporated $Au_{0.5}In_{0.5}$ with a T_c of 0.3 – 0.5 K, an *s*-wave superconductor, was found to yield a Josephson coupling with Sr_2RuO_4, probably because of the long superconducting coherence length it possess and its nice wetting properties on a polished Sr_2RuO_4 surface. In a more recent study, Al with a thin Ti underlay was also found to yield Josephson coupling with Sr_2RuO_4 through a ramp prepared by focused ion beam and low-energy Ar ion mill. Finally, in the original phase-sensitive experiment, an effort was made to avoid Ru inclusions, formed in the bulk during crystal growth with a varying density as discussed below, at the junction. The concern was that the presence of Ru inclusions at the junction interface may introduce uncertainties because the Ru part of the surface, which may function as a "short" for the Josephson coupling, tend to end up as a rounded shape with an ambiguous norm. Unfortunately, Ru inclusions appear to be present in

Sr_2RuO_4 crystals more often than expected, was difficult to avoid. Crystals from close to the surface of a single-crystal rod, which tends to be free of Ru inclusions were used. The polished crystal surface was examined under a high-magnifying-power optical microscope to make sure that Ru inclusions. The absence of Ru inclusions at the junction interface was further ensured by a careful screening of our devices through the detection of a feature, or features, in temperature dependence of the junction resistance, $R_j(T)$, between 1.5 and 3 K.

An experimental challenge to determine whether $I_c(\Phi=0)$ is a maximum or minimum is that the total amount of the flux threaded in the SQUID loop, Φ, may be different from the applied flux, Φ_{ext}, used in the experiment to modulate the critical current, I_c, To determine the true total flux threading a SQUID device, it was noted that

$$\Phi = \Phi_{ext} + \Phi_{ind} + \Phi_{trap} + \Phi_{bkgd} \qquad (4)$$

where Φ_{ind} is induced flux, in the absence of trapped flux, Φ_{trap}, and background flux, Φ_{bkgd} (minimized by careful magnetic shielding). For the GLB SQUID samples, $\Phi_{ind} = LI_{circ} = L(I_1 - I_2)$, where I_{circ} is the circulating current in the loop, and L is the self-inductance[65]. Φ_{ind} is determined by the sample size and the asymmetry of the SQUID. Early SQUID-based phase-sensitive experiments[66,67] on high-T_c relied on an extrapolation of R(H) measured at currents above I_c to zero current, an approach criticized by others[68] and apparently abandoned in favor of the beautiful corner junction experiments[69,70]. We adopted an alternative approach by showing that $I_c(\Phi_{ext}=0)$ corresponds to a minimum close to T_c of the SQUID, the lower one of the two junctions in the SQUID. In this case, $I_{circ} \rightarrow 0$, so that $\Phi = \Phi_{ext} + \Phi_{ind} \rightarrow \Phi_{ext}$, if $\Phi_{trap} = 0$. For a SQUID this leads to $2\pi m = \phi_1 - \phi_2 + (2\pi/\Phi_0)(\Phi_{ext} + \Phi_{ind} + \Phi_{trap})$, where m is an integer (or 0), ϕ_1 and ϕ_2 are phase drops across the two junctions in the SQUID. Clearly, ϕ_1 and ϕ_2, the two degrees of freedom of the system, can adjust themselves to accommodate any arbitrary amount of flux. To avoid trapped flux, another serious issue as trapped flux in a conventional SQUID could mimic the behavior of an unconventional SQUID as demonstrated in high-T_c work, we employed several strategies to detect and avoid trapped flux[71,72]. One can determine the actual field seen by the SQUID by examining the envelop of the $I_c(H)$ - the trapped flux always leads to an asymmetric $I_c(\Phi)$. It was found that warming up and cooling down the sample in zero field slowly in a controlled rate could prepare a trapped-flux-free SQUID state featuring a symmetric $I_c(\Phi)$, seen for example in Fig. 2C, which was used to determine whether $I_c(\Phi = 0)$ corresponds to a minimum or maximum as the T_c of the SQUID is approached.

Results of the phase-sensitive measurements on Sr_2RuO_4 were shown in Figs. 2C and D. Close to T_c, GLB SQUIDs were found to show a minimum while that of a control sample showed a maximum. This result, obtained in another sample, demonstrated that the phase of the order parameter changes by π after 180-degree rotation, suggesting that Sr_2RuO_4 is an odd-parity superconductor. Furthermore, results from a corner junction showed that the phase of the order parameter changes by $\pi/2$ after 90-degree rotation, consistent with the expectation of the p-wave pairing in Sr_2RuO_4. These results, together with the previous phase Josephson selection rule result discussed above, showed that the papring symmetry in Sr_2RuO_4 is that of Γ^-_5 state within the Rice-Sigrist scheme listed in Table 1.

As pointed outabove, Γ^-_5 state in Table 1 is chiral state featuring $k_x + i\,k_y$ or $k_x - i\,k_y$ domains. The results described above seem to suggest that a single domain, or in less likely scenario, odd number of domains, are prepared in our GLB SQUIDs. Given that our single-crystal-based GLB SQUID typically span a size as large as a mm, the domain size seem to be large, which is a point of current debate within the ruthenate research community. Experimentally, to address the issue on the possible presence of the domains, we employed a computer controlled, very slow (~ many hours) cool-down procedure to prepare a single domain state. The same procedure also helped ensure a trapped flux free sample. A symmetric quantum interference pattern would then be the signature of a single-domain, trapped-flux-free state.

4. Responses of bulk superconductivity to mechanical perturbations

4.1. Suppression of superconductivity by a hydrostatic pressure

Properties of Sr_2RuO_4 under a hydrostatic pressure were studied over the years. The earliest study was performed by Shirakawa *et al*. using relatively low quality crystal with T_c of ~ 0.9 K found that the T_c was suppressed by hydrostatic pressure at the rate of 0.3 K/GPa[73]. Since the maximum pressure they could reach is limited up to 1.2 GPa, it was not possible to suppressed T_c to 0 in this experiment. However, from the T_c suppression rate (*i.e.* 0.3 K/GPa) obtained in the low pressure range, the critical pressure for which T_c is suppressed to zero is expected to be ~3 GPa. The pressure dependence of the T^2 coefficient A of the in-plane resistivity $\rho_{ab} = \rho_0 + AT^2$, which is associated with quasiparticle effective mass, was found to change only slightly in the limited pressure range of their experiment. Yoshida *et al*. explored the pressure dependence of the normal-state properties of Sr_2RuO_4 and found that the temperature dependence of ρ_{ab} at low temperatures exhibited an evolution from Fermi liquid behavior of ~ T^2 at ambient pressure to ~ $T^{4/3}$ behavior as the pressure was raised to 8 GPa[74]. The $\rho \sim T^{4/3}$ behavior was found previously to result from 2D ferromagnetic fluctuations in the vicinity of the magnetic instability.

The 2D ferromagnetic fluctuation scenario was not confirmed by Shubnikov-de Haas oscillation measurements up to 3.3 GPa carried out by Forsythe *et al*. on high-quality crystals with a $T_c \sim 1.5$ K[24]. As shown in Fig. 3, T_c was found to be suppressed linearly by pressure, yielding a critical pressure where T_c vanishes to be ~ 7 GPa. Forsythe *et al.* also found that many-body enhancement of several parameters decreases with an increasing pressure. For example, A in the ρ_{ab} was found to decrease by ~ 45% and the quasiparticle effective mass, m*, extracted from the temperature dependence of the quantum oscillations dropped by 18%, 30% and 9% for α, β, and γ sheets of the Fermi surface, respectively, and attributed to weakened many-body interactions. The simultaneous decrease in T_c and m* with the increasing pressure suggests that electron-electron interaction plays a role in driving the superconductivity instability.

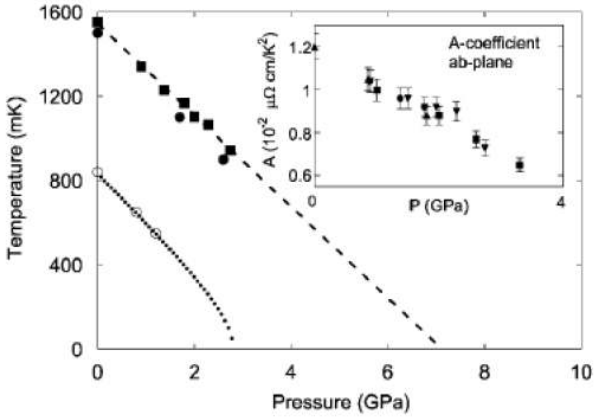

Figure 3. Hydrostatic pressure dependence of the superconducting transition temperature for Sr_2RuO_4. The inset shows the T^2 coefficient of in-plane resistivity as a function of pressure. Taken from Ref. 24.

Most interestingly, as the pressure is increased from ambient pressure to 3.3 GPa, the Fermi sheets, especially the γ sheet, were found to become increasingly 2D with decreasing k_z dependence. Considering that T_c deceases with the increasing pressure as well, it is reasonable to ask if interlayer coupling plays an role in the occurrence of superconductivity in Sr_2RuO_4 to begin with and whether the superconducting order parameter in the ambient pressure also depends on k_z. The answer to these questions will have implications on the pairing symmetry in the superconducting state.

4.2. Enhancement of superconductivity by a uniaxial stress

Nomura and Yamada explored the effects of an uniaxial stress applied along the *c* axis and found that it would lift the d_{xz} and d_{yz} bands, causing charge carriers from the these two bands to the d_{xy} band[75]. The Fermi level was in turn tpushed oward the van Hove sigularity, which leads to an increases the density of state at E_F and enhancment of T_c. on the other hand, Okuda *et al*. made a quantitative estimate for the T_c enhancement caused by uniaxial stress from their ultrasonic experiments combined with Ehrenfest relations[76] and obtained an uniaxial stress dependence of T_c with the form

$$(1/T_c)(dT_c/dP_{//[001]}) = + (0.7\pm0.2)\ \text{GPa}^{-1}, \qquad (5)$$

$$(1/T_c)(dT_c/dP_{//[100]}) = - (0.85\pm0.05)\ \text{GPa}^{-1}, \qquad (6)$$

where $P_{//[001]}$ and $P_{//[100]}$ represent uniaxial stress along the *c* and *a* axes, respectively. The positive sign on the right-hand side of Eq. 5 indicates that the uniaxial stress along the c axis would increase T_c, while the negative sign in Eq. 6 indicates that the in-plane uniaxial stress would decrease T_c. Note that Eqs. 5 and 6 are valid only in the elastic limit.

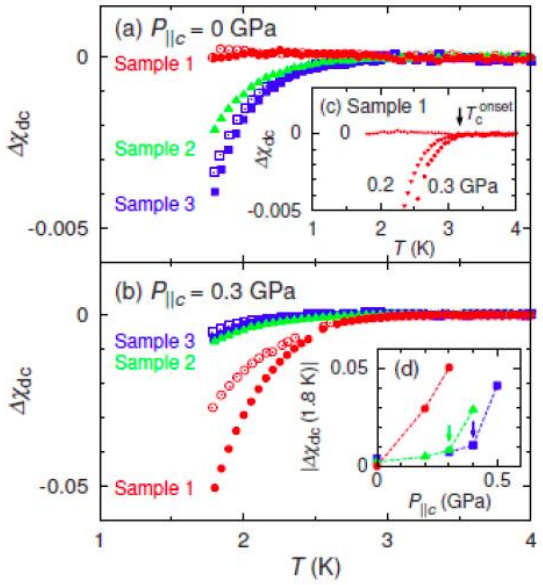

Figure 4. Temperature dependence of the dc susceptibility $\Delta\chi_{dc}$ of Samples 1 (circles), 2 (triangles), and 3 (squares) measured with 2 mT at P_c = 0 (a) and 0.3 GPa (b). Open and closed symbols indicate data taken in the FC and ZFC processes, respectively; c) Enlarged view near the onset for sample 1 at different P_c; d) Dependence of the dc shielding fraction on P_c at 1.8 K. The arrows indicate critical pressure P_c. Taken from Refs. 77 and 79.

Uniaxial stress measurements on Sr_2RuO_4 were performed by Kittaka *et al*. in which the uniaxial stress was applied along the *c* axis using a piston cylinder type pressure cell[77]. Both *dc* and *ac* susceptibility measurements on three samples under uniaxial stress. Under zero stress, Sample 1 is pure Sr_2RuO_4 with a very sharp superconducting transition at 1.34 K while Samples 2 and 3 contain a small amount of Ru inclusions which leads to a broad superconducting transition with the onset near 3 K (known as the 3-K phase[78]). As shown in Fig. 4, Sample 1 displays significant superconductivity enhancement under the *c*-axis uniaxial stress (P_c) with its T_c increasing from 1.34 K to 3.2 K as P_c is increased only to 0.2 Gpa. The superconducting fraction also increases rapidly with P_c. Samples 2 and 3 with Ru inclusions show much weaker shielding fraction enhancement, which indicates that the superconductivity enhancement is intrinsic property of Sr_2RuO_4. Such superconductivity enhancement caused by P_c in Sr_2RuO_4 is qualitatively consistent with the dependence of T_c on P_c (Eq. 5). However, the observed magnitude of T_c enhancement is much larger than that predicted by Eq. 5 in the elastic limit (~1

K/GPa). Electronic and magnetic properties of ruthenates are known to be sensitive to the rotation, tilting and flattening of the RuO_6 octahedra. Different from a hydrostatic pressure, an uniaxial stress along the *c* axis may trigger structural distrortion associated with RuO_2 octahedral, affecting the T_c of Sr_2RuO_4.

Although the piston-cylinder type pressure cell is effective in studying the *c*-axis uniaxial stress effects, it is difficult to apply this technique to study the in-plane uniaxial stress effect of pure Sr_2RuO_4 because the crystals tend to cleave. Kittaka *et al*.[79] found that this technique works well for the 3-K phase of Sr_2RuO_4-Ru eutectic system. For a crystal with onset T_c to ~3.5 K and the superconducting shielding fraction to ~0.5% at 1.8 K, the in-plane uniaxial stress was found to increase the shielding fraction at 1.8 K rises up to above 30% at a uniaxial stress of 0.4 GPa applied along either [100] or [110] direction even though the onset T_c remains nearly the same. In contrast, the increase of shielding fraction is relatively small (5% at 0.4 GPa) as the uniaxial stress is applied along the *c*-axis. These observations are surprising given that the superconductivity of Sr_2RuO_4 is expected to be suppressed by in-plane uniaxial stress as shown by Eq. 6 and was attributed to the stablization of lattice distortion by an in-plane uniaxial stress.

4.3. Enhancement of superconductivity by a uniaxial strain

If the pairing state of the bulk Sr_2RuO_4 indeed features a two-fold degeneracy, as in the Γ_5 state, the degeneracy will be lifted by in-plane uniaxial stress[80] , leading splitted superconducting transitions, with one shifting to a higher and the other to a lower temperature. Moreover, compressive and tensile stresses are expected to produce a symmetric response. Hicks *et al*. have recently developed a new apparatus to investigate in-plane uniaxial strain effect on the superconductivity of Sr_2RuO_4[81]. Their apparatus is composed of both extension and compression piezoelectric stacks, which allows to apply both compressive and tensile strains (ε) up to 0.23%. They conducted *ac* susceptibility measurements to determine T_c under uniaxial strain. Results on T_c as a function of ε are shown in Fig. 5. Compressive and tensile strains along the [100] direction were found to lead to strong, symmetric increase in T_c. In contrast, the T_c response to the strain applied along [110] direction is weaker and asymmetric. A cusp at $\varepsilon = 0$ expected theoretically for a $k_x + ik_y$ superconductor is not observed, however. More needs to be done to understand this interesting result.

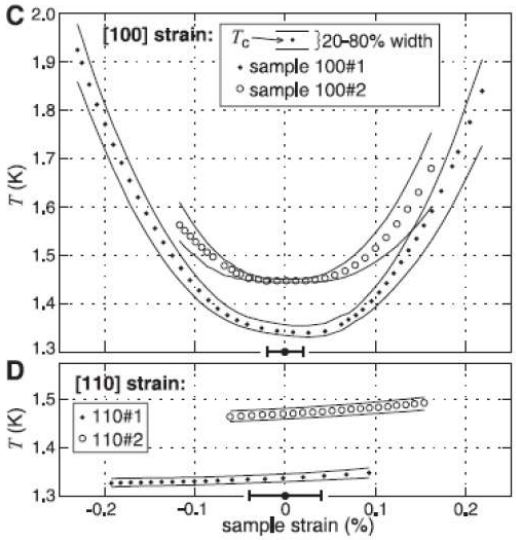

Figure 5. T_c as a function of strain along the [100] direction (upper panel) and the [110] direction (bottom panel) for Sr_2RuO_4. Taken from Ref. 81.

4.4. Symmetry lowering and the enhancement of T_c near a dislocation in Sr_2RuO_4

Recent work[82] revealed the presence of dislocations near an atomically sharp interface between Ru island and bulk Sr_2RuO_4 crystal in the utectic phase of Ru-Sr_2RuO_4 (the 3-K phase, see below), raising

the question as to how these dislocations could affect local superconductivity. A phenomenological theory was formulated to explore the effect of the loss of four-fold symmetry near a dislocation based on the analysis of the general free energy density of the bulk Sr_2RuO_4 with a four-fold tetragonal symmetry[83]. The symmetry lowering can due to the influence of an in-plane uniaxial stress/strain discussed, or the presence of an edge dislocation. A set of parameters, m_1 and m_2 used to quantify the effect of lattice distortions and μ to measure the mixing of the two order parameter components, can be introduced to describe the symmetry breaking strength. Following the idea of degenerate perturbation theory, the modified transition temperature T_{ch}, determined by the eigenvalues of the quadratic terms, is given by $T_{ch} = T_{c0} + \frac{1}{\alpha}(\sqrt{m_-^2 + |\mu|^2} - m_+)$

$$T_{ch} = T_{c0} + \frac{1}{\alpha}\left(\sqrt{m_-^2 + |\mu|^2} - m_+\right) \qquad (7)$$

where $m_\pm=(m_1 \pm m_2)/2$. Depending on the values of $m_\pm$ and μ, $T_{ch} > T_{c0}$ can be obtained. It is important that the asymmetry related terms m_- and μ always enhance the transition temperature, whereas the general level of the lattice distortion m_+ may either enhance or suppress the transition temperature.

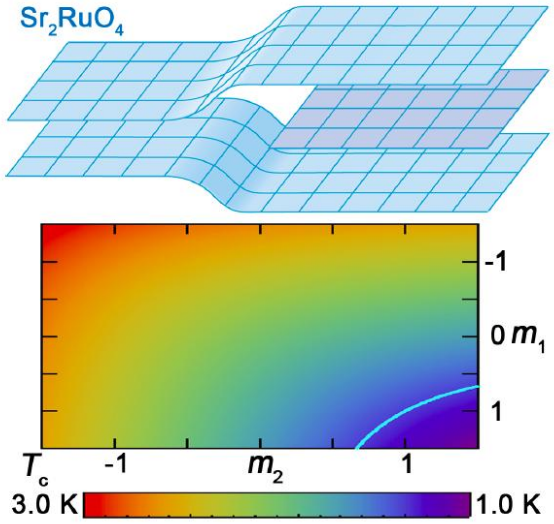

Figure 6. Upper pannel: Schematic showing an edge dislocation in Sr_2RuO_4. and the lost of four-fold symmetry. Lower panel: T_{ch} plotted as a function of $m_1/|\mu|$ and $m_2/|\mu|$ for $|\mu|/\alpha T_{c0} = 0.4$. The value of T_{ch} is represented by a color scale. The highlighted curve represents the contour of T_{ch} = 1.5 K. Taken from Ref. 83.

For a system featuring a single dislocation embedded in a bulk crystal of Sr_2RuO_4 with the dislocation line featuring a width d in the x direction, the locally enhanced superconducting transition temperature T_c is determined by T_{ch} (m_1, m_2, and μ) and the presence of the bulk. Solving the linearized Ginzburg-Landau equations derived from the general free energy density equation of bulk Sr_2RuO_4 and matching the boundary conditions at $x = 0$, T_c was obtained from the solution of

$$2\sqrt{\frac{K_2}{\alpha}(T_c - T_{c0})} = d(T_{ch} - T_c)\, 2\sqrt{\frac{K_2}{\alpha}(T_c - T_{c0})} = d(T_{ch} - T_c) \qquad (8)$$

which requires $T_{ch} > T_c > T_{c0}$ for self consistency. Both enhanced and suppressed local T_{ch} values a clearly possible (Fig. 6).

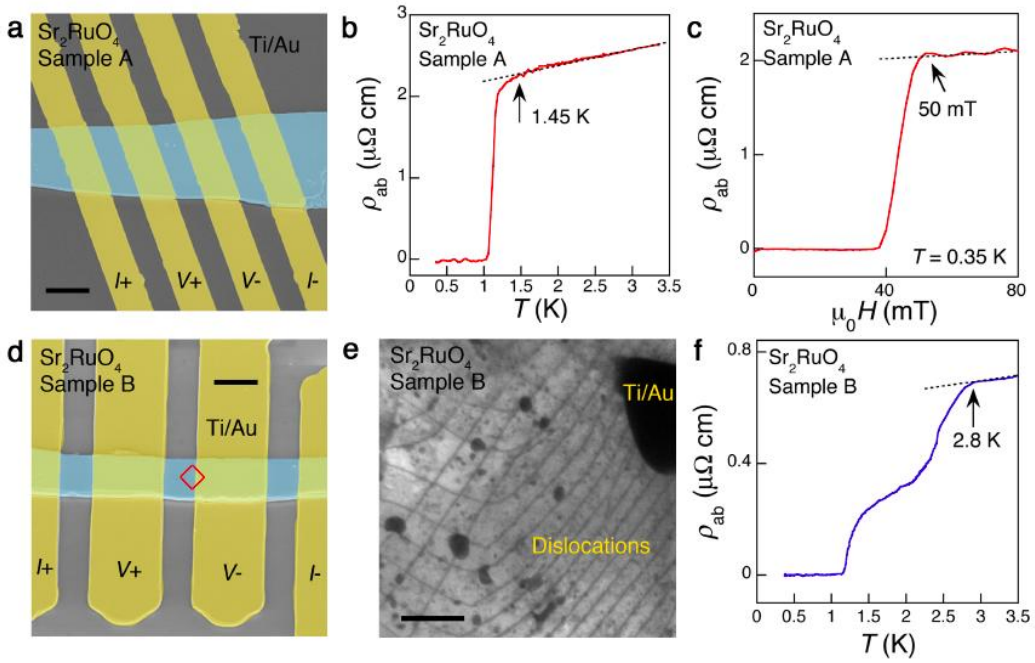

Figure 7. (**a**) False-color scanning electron microscopy (SEM) image of Sample A. The scale bar is 5 μm. (**b**) Temperature dependence of the in-plane resistivity ρ_{ab} for Sample A, taken at zero applied magnetic field. (**c**) Magnetic field dependence of ρ_{ab} for Sample A. (**d**) False-color SEM image of Sample B. The red square indicates the area examined by TEM. The scale bar is 5 μm. (**e**) TEM image of the boxed area in (**d**) for Sample B, showing dislocation lines but no Ru nanodomains. The scale bar is 200 nm. The regions not shown in this image were also checked by TEM and found to possess no Ru nanodomains. (**f**) Zero-field $\rho_{ab}(T)$ for Sample B. Taken from Ref. 83.

Electrical transport measurements on small crystals with dislocations were found to show an enhanced T_c (Fig. 7), providing direct experimental evidence for the enhanced superconductivity in Sr_2RuO_4 due to the presence of edge dislocation. While the microscopic origin of the T_c enhancement is not understood, it is reasonable to assume that near an edge dislocation, the interlayer coupling may be enhanced, which would lead to an enhanced T_c, as discussed above. Furthermore, if the pairing symmetry in Sr_2RuO_4 is indeed chiral *p*-wave, then edge states are expected[84], which may also lead to an increase in the density of states, and the enhancement of T_c.

5. Effects of crystal imperfections and superconductivity in non-bulk Sr_2RuO_4

5.1. Effects of crystal imperfections on superconductivity

The sensitivity of the occurrence of superconductivity in Sr_2RuO_4 to the presence of impurities was first established by Mackenzie *et al*.[36] who found that T_c, the residual in-plane resistivity ρ_{ab0}, and impurity concentrations (determined by chemical compositions analysis using electron probe microanalysis) of single crystals Sr_2RuO_4 were well correlated. In particular, crystals with a higher Al or Si concentration tend to possess a higher ρ_{ab0} and lower T_c. Specifically, crystals with a $\rho_{ab0} > 1.5$ μΩ cm containing around 300 - 450 ppm Al are non-superconducting whereas the crystals with $\rho_{ab0} < 0.5$ μΩ cm and $T_c > 1.3$ K contain < 30 ppm Al and Si. When ρ_{ab0} is increased above 1.1 μΩ cm where the mean free path l decreases to ~ 900 Å and the in-plane superconducting coherence length ζ_{ab} increases to ~910 Å, superconductivity becomes completely suppressed. Such dependence of T_c on ρ_{ab0} can be fitted very well to a modified Abrikosov and Gor'kov function[85, 86, 87]. Mao *et al.* found similar suppression of superconductivity by impurities[88]. Measurements on superconductivity in several intentionally doped

systems, including $Sr_{2-y}La_yRuO_4$[89] and $Sr_2Ru_{1-x}M_xO_4$ (M = Ti, Ir)[90,91], show that chemical dopants in these systems showed different effects. Here La^{3+} and Ti^{4+} are nonmagnetic while Ir^{4+} is magnetic. Furthermore, La^{3+} is an out-of-plane dopant, where Ti^{4+} and Ir^{4+} are in-plane dopants. It was found that La^{3+} is less effective in increasing resistivity than Ti^{4+} and Ir^{4+}. On the other hand, the variation of T_c with ρ_{ab0} for all these doped systems follows the Abrikosov and Gor'kov curve, suggesting that non-magnetic and magnetic impurities have similar pair-breaking effects.

The level of crystal defects in bulk Sr_2RuO_4, which dependent on crystal growth condition, in particular, the crystal growth speed, have similar effect on the T_c of Sr_2RuO_4. Indeed, crystals grown at the speed above 5 cm/h usually have a high level of defects and lower T_c while the crystals with the highest T_c ($\approx$ 1.5 K) were usually grown with a speed in the 4-4.5 cm/h range[88,92]. Moreover, the value of T_c could be increased by annealing at high temperatures for crystals with relatively low T_c but not those that already achieving a T_c near the optimal. Interestingly, the variation of T_c with ρ_{ab0} was found to also follow the same modified Abrikosov and Gor'kov function when ρ_{ab0} was mainlly determined by crystal defects, clearly indicates crystal defects suppresses the T_c of Sr_2RuO_4 just like the impurities.

The surface of the *ab* face of Sr_2RuO_4 prepared by room-temperature cleaving were found to be non-superconducting, presumably due to the rotation of the RuO_6 octahedra at the surface[18]. Inside the bulk, these RuO_6 octahedra are not expected to be subjected to any rotation and tilting, yielding a relatively stiff structure. However, an scanning tunneling microscopy and scanning tunneling spectroscopy (STM/STS) study revealed the absence of superconductivity on crystal surface made by *in situ* low-temperature cleaving where the rotation of RuO_6 octahedra does not occur[93]. Superconductivity was detected even though the topography was unusual, whose origin was not understood.

5.2. Epitaxial films of Sr_2RuO_4 grown by pulsed laser deposition

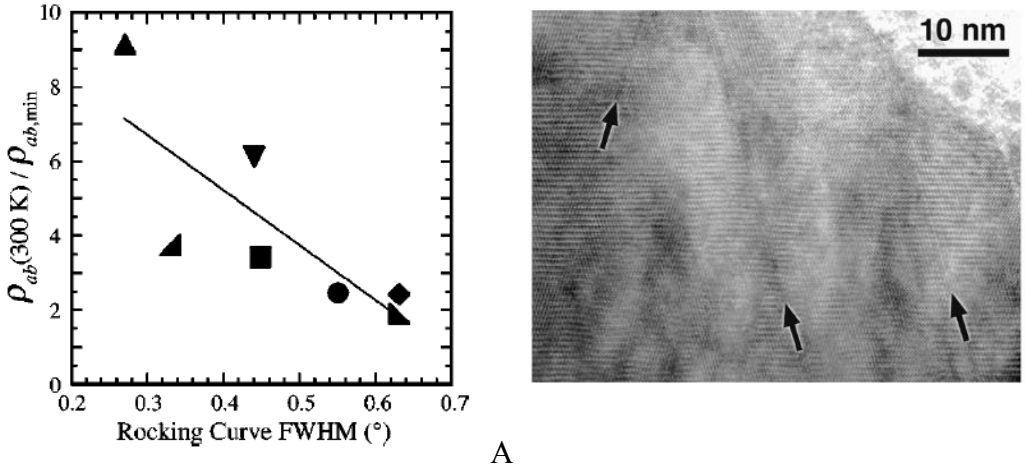

Figure 8. A) Full width at half maximum (FWFM) of X-ray diffraction rocking curve *vs*. the residue resistivity ratio (RRR) for pulsed laser deposition grown films of Sr_2RuO_4 with ~99.98% pure target; B) High-resolution transmission electron microscopy (HRTEM) of a high purity film. Stacking faults as dominant structural defects are shown. Taken from Ref. 95.

Superconducting thin films of Sr_2RuO_4 are highly desirable for certain for experiments such as phase sensitive measurements as well as possible practical use of this superconducting material. However, the demand on the level of structural perfection in films of Sr_2RuO_4 has proved to be difficult to fulfill. Single-domain, *c*- and *a*-axis oriented epitaxial films of Sr_2RuO_4 were grown by pulsed laser deposition by the mid of 1995 using a target of a stoichiometric proportion of $SrCO_3$ (99% pure) and RuO_2 (99.9% pure)[94]. Results from θ-2θ and ϕ scans of X-ray diffraction indicate epitaxial alignment of the film and substrate in-plane axes in both growths. Electrical transport measurements showed that these films were

non-superconducting. Taking hints from the study of effect of impurities on the superconducting T_c of Sr_2RuO_4 in the bulk, the early effort was concentrated in reducing the impurity level in the target. However, epitaxial Sr_2RuO_4 thin films deposited from a ~99.98% purity target were also found to be not superconducting[95]. Interestingly, the width of the X-ray diffraction rocking curve and the residue resistivity ratio of the Sr_2RuO_4 film were found to be correlated (Fig. 8A), suggesting that the structural perfection is the main source of the electron scattering in these films. High-resolution transmission electron microscopy revealed that the dominant structural defects, *i.e.*, the defects leading to the observed variation in rocking curve widths in the films, are {011} planar defects (Fig. 8B), with the averaged spacing comparable to or smaller than the zero-temperature in-plane superconducting coherence length of Sr_2RuO_4, $\xi_{ab}(0)$, suggesting that minimizing structural disorder is the key challenge to achieving superconducting Sr_2RuO_4 films.

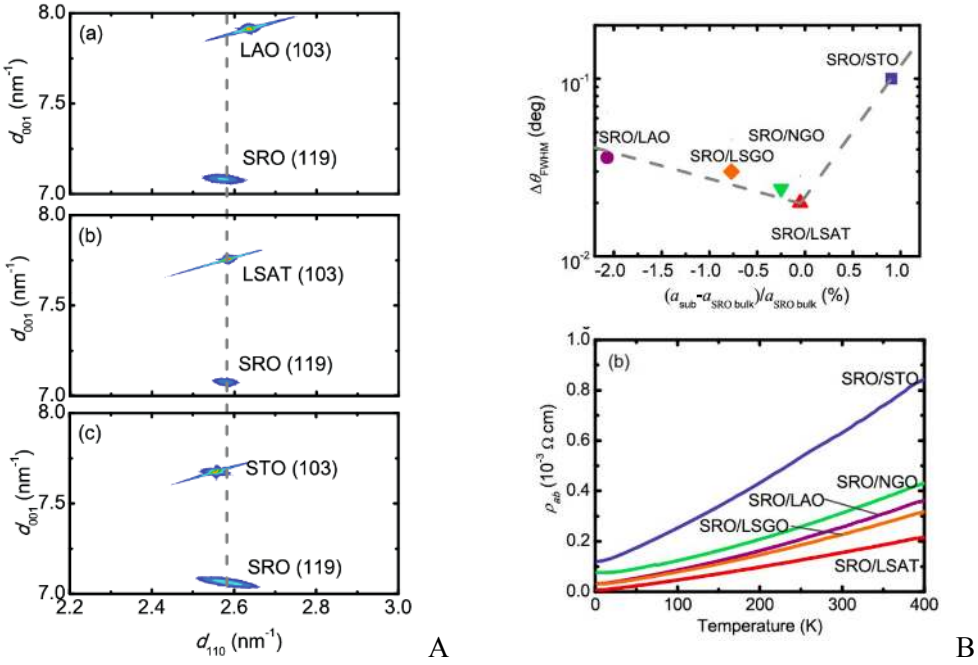

Figure 9. A) High-resolution four-circle X-ray diffraction reciprocal space maps (RSMs) of around (119) reflections of epitaxial Sr_2RuO_4 films grown on (001) surface of (a) LAO ($LaAlO_3$), (b) LSAT [$(LaAlO_3)_{0.3}(SrAl_{0.5}Ta_{0.5}O_3)_{0.7}$], and (c) STO ($SrTiO_3$) substrates; B) Upper panel: $\Delta\theta_{FWHM}$, the FWHM of the Sr_2RuO_4 (002) rocking curve, as a function of the lattice mismatch for Sr_2RuO_4 films on various substrates as indicated, where a_{sub} and $a_{SRO\ bulk}$ are lattice constants of the substrate and the bulk Sr_2RuO_4, respectively; Lower panel: ρ_{ab} *vs*. T for Sr_2RuO_4 films grown on various substrates as indicated. For the film grown on LSAT, the residual resistivity is 6 μΩ cm and the RRR ($\rho_{ab,\ 300\ K}/\rho_{ab,\ 2\ K}$) is ~25. Taken from Ref. 96.

Recent efforts[96] in the growth of epitaxial thin films of Sr_2RuO_4 by pulsed laser deposition were made in Mao group using high-purity, single-crystal $Sr_3Ru_2O_7$ grown by the floating zone method as the target. The use of single crystals of $Sr_3Ru_2O_7$ rather than Sr_2RuO_4 as the target allows excess Ru in the target to compensate its loss during the growth of Sr_2RuO_4 films. High-resolution four-circle X-ray diffraction reciprocal space map (RSM) measurements on the single (119) diffraction of the Sr_2RuO_4 film were performed to characterize the structure of the films grown on various substrates. From the horizontal and vertical peak positions in the RSM, both lattice parameters, *a* and *c*, as well as the epitaxial strain of the film along in-plane crystallographic directions can be calculated. Surprisingly, the Sr_2RuO_4 (119) diffraction spots of films grown on different substrated were found to locate at essentially the same position along the horizontal direction in RSM (Fig. 9A), a signature of strain relaxation. The in-plane

lattice constant, *a*, of these films are found to be nearly identical to that of bulk Sr_2RuO_4 even though a 0.05 – 2.1% difference in *a* between bulk Sr_2RuO_4 and the substrate is present. One of the substrates, LSAT, has the least difference (0.05%) in the lattice constant from bulk Sr_2RuO_4. The (119) diffraction spot of the film grown on LSAT appears to be nearly aligned with the LSAT (103) spot.

Interestingly, FWFM of the rocking curve of the Sr_2RuO_4 (002) reflection of Sr_2RuO_4 films grown on various substrate, $\Delta\theta_{FWHM}$, was found to still vary with the lattice mismatch(Fig. 8B) where the smallest $\Delta\theta_{FWHM}$ (~ 0.02°) was found in Sr_2RuO_4 films grown on LSAT featuring the least lattice mismatch. Since $\Delta\theta_{FWHM}$ characterizes the crystalline mosaic spread of the films, the substrate dependence of $\Delta\theta_{FWHM}$ in Fig. 10B is an measure of the non-flat deformation of the film caused by lattice mismatch. Similar to the previous finding shown in Fig. 8A, the residual resistivity and RRR of the Sr_2RuO_4 films seem to correlated with $\Delta\theta_{FWHM}$ well with the Sr_2RuO_4 film grown on LSAT showing the smallest residual resistivity of 6 μΩ cm with a RRR ≈ 25. Unfortunately, even for these films showing such a low residual resistivity, electrical transport measurement carried out down to mK range in a dilution refrigerator did not show superconductivity.

A single success in the growth of superconducting films of Sr_2RuO_4 was reported[97]. In this case, the epitaxial film of Sr_2RuO_4 were grown in an ultra-high vacuum PLD chamber using a modestly high purity target (made from 99.99% pure $SrCO_3$ and 99.9% pure RuO_2) on a LSAT substrate. While the growth was done under conditions not so different from other attempts, refelcted high energy electron diffraction (RHEED) was used to monitor the growth. The target was polished after each run since the surface was decomposed into species including metallic Ru. The X-ray diffraction studies showed a *c*-axis oriented epitaxial structure of Sr_2RuO_4 with lear Laue fringes are observed. The FWHM of **(**006**)** rocking curve was found to be as narrow as 0.02° for films grown with RHEED oscillations. The X-ray diffraction RSM of the film indicated pseudomorphic in-plain lattice structure. In addition, TEM studies revealed crystalline defects similar to those observed previously (Fig. 10A). However, areas free from these defects much larger than $\xi_{ab}(0)$. The films was found to show a residual resistivity of 2.3 μΩ cm, a $\rho_{300\,K}/\rho_{2\,K} \approx 82$, and a superconducting transition with a zero resistivity at 0.6 K (Fig. 10B), both of which were indeed the best reported. Unfortunately, the growth of superconducting films of Sr_2RuO_4 has not been reproduced, evidently not even by the same group reporting the successful growth to begin with.

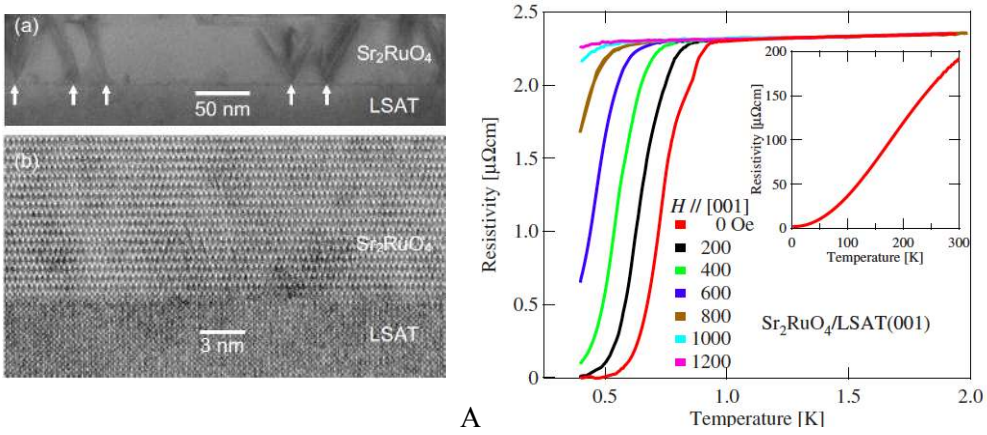

A B

Figure 10. A) Cross sectional TEM images. Arrows in **(a)** indicate planar defects due to out-of-phase boundaries. High resolution image in **(b)** shows coherent connection of both lattices; (B) Resistivity as a function of temperature below 2 K under various magnetic fields applied parallel to the *c* axis of the film. Inset shows resistivity as a function of temperature at higher temperatures. Taken from Ref. 97.

5.3. Eutectic phase of Ru/Sr_2RuO_4

The eutectic system of Ru-Sr_2RuO_4 consists of microdomains of pure Ru metal embedded in a bulk single crystal of Sr_2RuO_4. In the synthesis of superconducting Sr_2RuO_4 single crystals by the floating zone method, the high volatility of Ru leads to Ru loss during the growth. Excessive RuO_2 is then added to the feed rod, resulting in the formation of Ru microdomains. These Ru microdomains were found to be superconducting with a T_c as high as 3 K - thus referred to as the 3-K phase[78]. A phenomenological theory was put forward[98] to explain the enhancement of superconductivity. In this picture, a single-component *p*-wave wave function with its positive and negative lobes parallel to the interface (say, k_y-state) will nucleate below the onset of the 3-K phase, with the two-component $k_x \pm ik_y$ state emerges only when the temperature is below a characteristic temperature, T^*, which is higher than the bulk T_c.

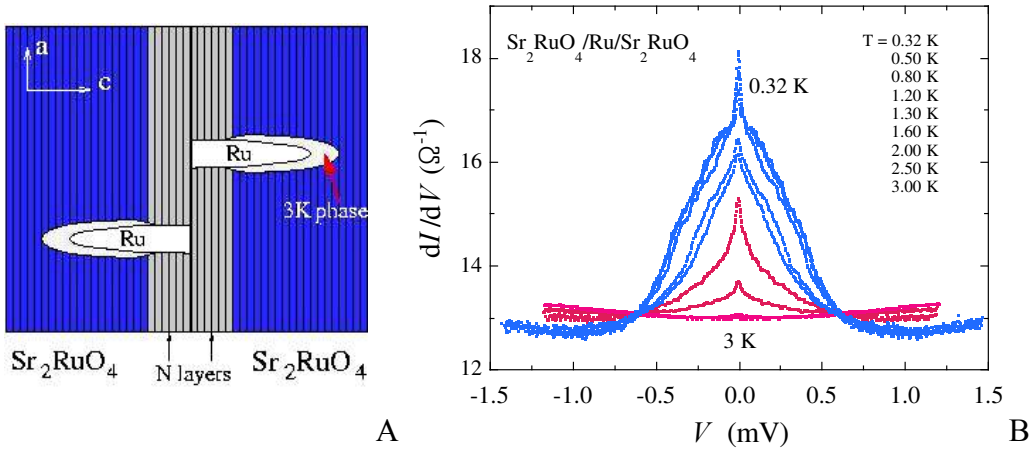

Figure 11. A) Schematic of a Sr_2RuO_4-Ru-Sr_2RuO_4 "break junction". The cleaved surface is non-superconducting, resulting a normal (N) layer; B) Tunneling spectra at various temperatures as indicated. Taken from Refs. 16 and 39.

Single quasiparticle tunneling were carried out in a "break junctions" of Sr_2RuO_4-Ru-Sr_2RuO_4 prepared by cleaving a Ru containg single crystal of Sr_2RuO_4 and then holding two cleaved pieces back together, resulting in a junction shown schematically in Fig. 11A[99]. Results obtained in these measurements revealed the presence of Andreev surface bound states (ABSs). It is known that at the surface of a non-*s*-wave superconductor, the intrinsic orientation dependence of the phase of the order parameter results in mid-gap Andreev bound states and an associated zero-bias conductance peak (ZBCP) in the tunneling spectrum[100], providing information on the pairing symmetry of the superconductor, as done in high-T_c cuprates[101,102] and the bulk phase of Sr_2RuO_4[38]. The tunneling spectra showed different characteristics below and above the T_c of the bulk phase, T_{cb} (Fig. 10B). These results are consistent with the phenomenology that the 3-K phase is non-*s*-wave, with a pairing state different from that in the bulk above the bulk T_c, and at low temperatures, a chiral *p*-wave state is realized. In addition, the tunneling spectra at low temperature is consistent with an order parameter featuring k_z-dependence with horizontal line nodes[103].

A high resolution transmission electron microscopy (HRTEM) study revealed the interface between the Ru island and the bulk Sr_2RuO_4 is atomically sharp, terminated uniformly by a Sr/O layer on the Sr_2RuO_4 side[82]. Furthermore, scanning Raman spectroscopy measurements on the area surrounding a Ru island revealed that, a change of the spectrum near the Ru-Sr_2RuO_4 interface[82]. The P_1 peak (vibration of Sr ions) and the P_2 peak (vibration of apical oxygen), both along the **c** axis were found to shift to high frequencies as the interface is approached, suggesting significant phonon hardening, which was found over the entire interface region surrounding a Ru island. The consequences of the atomically sharp interface as well as the phonon hardening at the interface have not been clarified. Finally, single particle tunneling into the mecahnically polished surface of Ru detect a superconducting energy gap only below

the intrinsic T_c for Ru, 0.5 K, corresponding to the T_c of pure bulk Ru, suggesting that superconducting energy gap induced by proximity effect does not survice at the surface of Ru even if it is present below T_c in the interior of the island in pure Ru.

5.3. Mesoscopic size Sr_2RuO_4 and the existence of half-flux-quantum states

Spin-triplet superconductivity supports novel topological objects, such as half-flux-quantum ($h/4e$) vortices and the associated Majorana modes[104,105], the zero-energy state in the core of a half-flux-quantum vortex found in a chiral *p*-wave superconductors. Majorana modes carry the exotic non-Abelian statistics and are useful for fault-tolerant topological quantum computing[106]. Unfortunately, the half-flux-quantum vortices are in general not stable while in mesoscopicform, they are. Recently, half-height magnetization steps were found in a cantilever magnetometry measurement on mesoscopic sized, doubly connected Sr_2RuO_4 (Fig. 12A)[107]. Specifically, transitions between integer fluxoid states and half-integer transitions marked by steps in the magnetization with half the height of the ones between integer fluxoid states. These half-height steps are consistent with the existence of a half-flux-quantum ($\Phi_0/2 = h/4e$) state in Sr_2RuO_4.

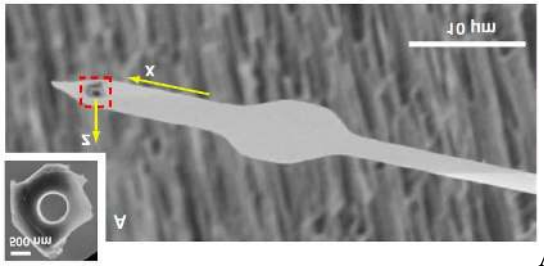

A

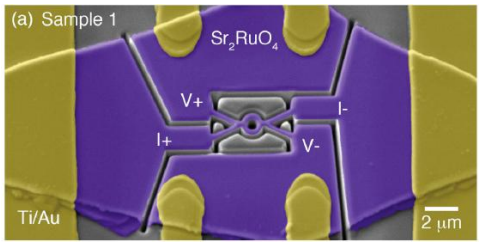

B

Figure 12. A) Candilever with a mesoscopic sized, doubly connected Sr_2RuO_4 attached to it. Taken from Ref. 107); B) False-color SEM image of a mesoscopic sized ring of Sr_2RuO_4 crystal, the Ti/Au lead (yellow), and the ring device (blue). Taken from Ref. 108.

Little-Parks resistance oscillation measurements on superconducting mesoscopic rings of Sr_2RuO_4 have been carried out[108] in order to obtain additional, independent evidence for the existence of half-flux-quantum state in Sr_2RuO_4. Because superconducting films of Sr_2RuO_4 are not yet available, develop a technique to prepare mesoscopic rings of Sr_2RuO_4 using thin, flat crystals that are in turn prepared by mechanical exfoliation from bulk single crystals. We use photolithography to prepare the leads needed for the Little-Parks resistance oscillation measurements and focused ion beam to cut the ring (Fig. 11B). Applying a magnetic field perpendicular to the plane of the ring (along the *c* axis) without the in-plane magnetic field that was used in the cantilever experiment, we found pronounced resistance oscillations of full flux quantum, Φ_0. Half-height magnetization jumps near half-flux quanta seen in the presence of an in-plane field would imply the splitting of the resistance peaks. Such a pattern of resistance oscillations have not been observed in our measurements at the time of this writing even when an in-plane field was applied.

6. Additional unresolved issues

In addition to important issues discussed above, other issues are yet to be resolved. First, whether nodes in the order paramer are present is not resolved. Part of the difficulty originates from the multiple bands of the elctronic states in Sr_2RuO_4. The Γ^-_5 state in a single-band superconductor would feature an isotropic, nonzero gap in the bulk with gapless chiral edge states on the surface, forming a topological superconductor. In principle, the order parameter can possess either horizontal nodes by making the order parameter depend on k_z in addition to k_x and k_y or vertical nodes with no k_z dependence[109,110,111,112,113], while keeping the essential feature of the Γ^-_5 state. The multiband nature of the Fermi surface for Sr_2RuO_4 consisting of three cylindrical sheets from α, β, and γ but bands, however, makes it possible to account

for the power-law behavior without invoking nodes. Indeed, the amplitude as well as the phase of the order parameter can be different on different bands, characteristic features of orbital dependent superconductivity. For Sr_2RuO_4, the order parameter was suggested to be large on γ but tiny on α and β sheets[114] or the other way around.

Second, whether domains and domain walls exist in Sr_2RuO_4 need to be resolved. In addition to chiral surface currents, the Γ^-_5 state should also feature domains and domain walls, which have not been imaged directly. WE should continue to work on this specific issue using Josephson tunneling as a probe, which has already been shown to be effective. The chiral *p*-wave Γ^-_5 state will leads to domains of degenerate $k_x + i\, k_y$ and $k_x - i\, k_y$ states and domain walls between the two neighboring domains. A domain wall terminates at the surface. A Josephson junction covering even or odd number of domains and domain walls between them are expected to show different patterns of quantum oscillations. Experiments on this and other sample configurations are need to obtain a coherent picture that will reconcile results suggesting that Sr_2RuO_4 has a pairing state of Γ^-_5 and those indicating that the chiral surface currents could not be detected.

Third, the mechanism of superconductivity in Sr_2RuO_4 is not yet understood. Models based on ferromagnetic fluctuation[115], antiferromagnetic fluctuation[116], spin-orbital coupling[117], or Hund's rule coupling[10], have been proposed. Electron-phonon interaction and Coulomb repulsion are all eelevant to the occurrence of superconductivity. The study of the eutectic phase of Ru-Sr_2RuO_4 will not only provide insight into the mechanism of superconductivity in Sr_2RuO_4 because of the unexpected enhancement of superconductivity, but also help understand some fundamental issues associated with spin-triplet superconductors such as interfacial superconductivity and *p*-wave proximity effec.

Finally, superconducting films of Sr_2RuO_4 need to be grown in a reproducible manner. The availability of these films will help resolve issues discussed above, including next-generation phase-sensitive measurements for pinning down the precise pairing symmetry using experimental design parallel with the tricrystal experiments in the high-T_c work. Even though some barriers created by the lack of superconducting thin films of Sr_2RuO_4 can be overcome by the use of mechanically exfoliated thin crystals, the growth of superconducting thin films of this material will open doors for possible applications of this material. Given that growing thin films of Sr_2RuO_4 has become such a material engineering challenge, progress in this area may also bring about technological breakthroughs in the synthesis of ultraclean materials of complex oxides.

6. Summary and outlook

Superconductivity in Sr_2RuO_4 has been discovered for a little over 20 years. Much progress has been made towards understanding the nature of superconductivity in this materials during these years. In this brief review, we discussed various unconventional aspects of superconductivity including features on the symmetry and the mechanism of the pairing and data supporting unconventional pairing symmetry in this material, focusing in particular on issues that will likely to remain a subject of active research in coming years. The phase-senistive measurements that have provided strong support for odd-parity, spin-triplet superconductivity in Sr_2RuO_4, which will also help pin down the precise form of the order parater and the search for the direct evidence for the chiral superconductivity, are discussed in some detail. The responses of superconductivity to the mechanical perturbations should help understand the mechanism of superconductivity in Sr_2RuO_4, even though solving this problem will probably remain a big challenge for some time. Finally, discussion on non-bulk Sr_2RuO_4 with many unusual features, which should represent growing areas of future research, is also meant to highlight the highly unconventional nature of the superconductivity in this material.

Even though several important issues remain to be resolved in order for a coherent picture on the pairing symmetry in Sr_2RuO_4 to be settled, as discussed above, there has been growing sense that the pairing symmetry in this material is unconventional, non-*s*-wave, and most likely spin-triplet. It is crucial

that several important but difficult experiments on Sr_2RuO_4 be carried out, which will help resolve the issues presented above and make this material system a testing ground for exploring consequences of this novel pairing symmetry and the possible use of such a superconductor.

Acknowledgements

We would like to thank R. Cava, K. Hasselbach, H-Y. Kee, J. Kirtley, Y. Maeno, K. Moler, D. Shen, S. Wang, Z. Wang, Y. Xin, Z. Xu, C-C. Tsuei, J. Wei for collaboration, graduate students K. Nelson, Y.A. Ying, X, Cai, S. Mills, and B. Zarkrewski for the their work and collaboration, D.F. Agterberg, S-K. Chung, V. B. Geshkenbein, J. K. Jain, C. Kallin, A. J. Leggett, T. M. Rice, J. A. Sauls, M. Sigrist, D. J. van Harlingen, and S-K. Yip for useful discussions. The work done at Penn State is supported by DOE under Grant No. DE-FG02-04ER46159, at SJTU by Ministry of Science and Technology of China (Grant 2012CB927403), and at Tulane by NSF under DMR-1205469.

References

1. J. Bardeen, L. N. Cooper, J. R. Schrieffer, "Theory of superconductivity," Phys. Rev. 108, 1175 (1957).

2. V. M. Edelstein, "Triplet superconductivity and magnetoelectric effect near the *s*-wave-superconductor-normal-metal interface caused by local breaking of mirror symmetry," Phys. Rev. B 67, 020505 (2003).

3. V. P. Mineev and M. Sigrist, " Non-centrosymmetric superconductors: Introduction and overview," Lecture Notes in Physics, v. 847, Editors: Ernst Bauer and Manfred Sigrist, Springer (2012).

4. V. P. Mineev and K.V. Samokhin, "Introduction to unconventional superconductivity," Gordon and Breach Science Publishers (1999).

5. J. J. Randall and R. Ward, "The preparation of some ternary oxides of the platinum metals," *J. Am. Chem Soc.* 81, 2629–2631 (1959).

6. F. Lichtenberg, A. Catana, J. Mannhart, and D.G. Schlom, "Sr_2RuO_4: A metallic substrate for the epitaxial growth of $YBa_2Cu_3O_{7-\delta}$," Appl. Phys. Lett. 60, 1138 (1992).

7. R. J. Cava, B. Batlogg, K. Kiyono, H. Takagi, J. J. Krajewski, W. F. Peck, Jr., L. W. Rupp, Jr., and C. H. Chen, "Localized-to-itinerant transition in $Sr_2Ir_{1-x}Ru_xO_4$," Phys. Rev. B 49, 11890 (1994).

8. Y. Maeno, H. Hashimoto, K. Yoshida, S. Nishizaki, T. Fujita, J. G. Bednorz, and F. Lichtenberg, "Superconductivity in a layered perovskite without copper," Nature 372, 532 (1994).

9. T. M. Rice and M. Sigrist, "Sr_2RuO_4: An electronic analogue of ^{3}He?" J. Phys.: Condens. Matter 7, L643 (1995).

10. G. Baskaran, "Why is Sr_2RuO_4 not a high T_c superconductor? Electron correlation, Hund's coupling and *p*-wave instability," Physica B 223&224, 490 (1996).

11. A. P. Mackenzie and Y. Maeno, "The superconductivity of Sr_2RuO_4 and the physics of spin-triplet pairing," Rev. Mod. Phys 75, 657 (2003).

12. Y. Maeno, S. Kittaka, T. Nomura, S. Yonezawa, and K. Ishida, "Evaluation of spin-triplet superconductivity in Sr_2RuO_4," J. Phys. Soc. Jpn. 81, 011009 (2012).

13. Y. Maeno, T. M. Rice, and M. Sigrist, " The intriguing superconductivity of strontium ruthenate," Phys. Today 1, 42 (2001).

14. C. Bergemann, A. P. Mackenzie, S. R. Julian, D. Forsythe, and E. Ohmichi, " Quasi-two-dimensional Fermi liquid properties of the unconventional superconductor Sr_2RuO_4," Adv. Phys. 52, 639–725 (2003).

15. I. Eremin, D. Manske, S. G. Ovchinnikov, and J. F. Annett, " Unconventional superconductivity and magnetism in SrRuO and related materials," Ann. Phys. (Leipzig) 13, 149 – 174 (2004).

16. Y. Liu, "Phase-sensitive-measurement determination of odd-parity, spin-triplet superconductivity in Sr_2RuO_4," New. J. Phys. 12075001 (2010).

17. C. Kallin, " Chiral *p*-wave order in Sr_2RuO_4," Rep. Prog. Phys. 75, 042501 (12pp) (2012).

18. R. Matzdorf, Z. Fang, Ismail, J. Zhang, T. Kimura, Y. Tokura, K. Terakura, and E. W. Plummer, "Ferromagnetism stabilized by lattice distortion at the surface of the *p*-wave superconductor Sr_2RuO_4," Science 289, 746 (2000).

19. Y. Liu, K. D. Nelson, Z. Q. Mao, R. Jin, and Y. Maeno, "Tunneling and phase-sensitive studies of the pairing symmetry in Sr_2RuO_4," J. Low Temp. Phys. 131, 1059 (2003).

20. T. Oguchi, "Electronic band structure of the superconductor Sr_2RuO_4," Phys. Rev. B 51, R1385 (1995).

21. D. J. Singh, "Relationship of Sr_2RuO_4 to the Superconducting Layered Cuprates," Phys. Rev. B 52, 1358 (1995).

22. A. P. Mackenzie, S. R. Julian, A. J. Diver, G. J. McMullan, M. P. Ray, G. G. Lonzarich, Y. Maeno, S. Nishizaki, and T. Fujita, "Quantum oscillations in the layered perovskite superconductor Sr_2RuO_4," Phys. Rev. Lett. 76, 3786 (1996).

23. A. Damascelli, D. H. Lu, K. M. Shen, N. P. Armitage, F. Ronning, D. L. Feng, C. Kim, Z.-X. Shen, T. Kimura, Y. Tokura, Z. Q. Mao, and Y. Maeno, "Fermi surface, surface states, and surface reconstruction in Sr_2RuO_4," Phys. Rev. Lett. 85, 5194 (2000).

24. D. Forsythe, S. Julian, C. Bergemann, E. Pugh, M. Steiner, P. Alireza, G. McMullan, F. Nakamura, R. Haselwimmer, I. Walker, S. Saxena, G. Lonzarich, A. Mackenzie, Z. Mao, and Y. Maeno, "Evolution of Fermi-Liquid Interactions in Sr_2RuO_4 under Pressure," *Phys. Rev. Lett*. 89, 166402 (2002).

25. I. Zutic and I. Mazin, "Phase-sensitive test of the pairing state symmetry in Sr_2RuO_4," Phys. Rev. Lett. 95, 217004 (2005).

26. M. W. Haverkort, I. S. Elfimov, L. H. Tjeng, G. A. Sawatzky, A. Damascelli, "Strong spin-orbit coupling effects on the Fermi surface of Sr_2RuO_4," Phys. Rev. Lett. 101, 026406 (2008).

27. A. J. Leggett, "A theoretical description of the new phases of liquid ^{3}He," Rev. Mod. Phys. 47, 331 (1975).

28. Z-Q. Mao, Y. Maeno, Y. Mori, S. Sakita, S. Nimori, and M. Udagawa, " Sign reversal of the oxygen isotope effect on T_c in Sr_2RuO_4," Phys. Rev. B63, 144514 (2001).

29. S. NishiZaki, Y. Maeno, and Z. Mao, "Effect of impurities on the specific heat of the spin-triplet superconductor Sr_2RuO_4," J. Low Temp. Phys. 117, 1581 (1999).

30. I. Bonalde, B. D. Yanoff, M.B. Salamon, D. J. van Harlingen, E. M. E. Chia, Z-Q. Mao, and Y. Maeno, "Temperature dependence of the penetration depth in Sr_2RuO_4: Evidence for nodes in the gap function," Phys. Rev. Lett. 85, 4775 (2000).

31. K. Izawa, H. Takashashi, H. Ymaguchi, Y. Matsuda, M. Suzuki, T. Sasaki, T. Fukase, Y. Yoshida, R. Settai, and Y. Onuki, "Superconducting gap structure of spin-triplet superconductor Sr_2RuO_4 studied by thermal conductivity," Phys. Rev. Lett. 86, 2653 (2001).

32. M. A. Tanatar, M. Suzuki, S. Nagai, Z.Q. Mao, Y. Maeno, and T. Ishiguro, "Anisotropy of magnetothermal conductivity in Sr_2RuO_4," Phys. Rev. Lett. 86, 2649 (2001).

33. C. Lupien, W.A. MacFarlane, C. Proust, L. Taillefer, Z.Q. Mao, and Y. Maeno, "Ultrasound Attenuation in Sr_2RuO_4: An angle-resolved study of the superconducting gap function," Phys. Rev. Lett. 86, 5986 (2001).

34. K. Ishida, Y. Kitaoka, K. Asayama, S. Ikeda, S. Nishizaki, Y. Maeno, K. Yoshida, and T. Fujita, "Anisotropic pairing in superconducting Sr_2RuO_4: Ru NMR and NQR studies," Phys. Rev. B 56, R505-R508 (1997).

35. R. Jin, Y. Zadorzhny, D. G. Schlom, Y. Mori, Y. Maeno, and Y. Liu, "Observation of anomalous temperature dependence of the critical Current in Pd/Sr_2RuO_4/Pb junctions," Phys. Rev. B 59, 4433-4438 (1999).

36. A. P. Mackenzie, R. K. W. Haselwimmer, A. W. Tyler, G. G. Lonzarich, Y. Mori, S. Nishizaki, and Y. Maeno, "Extremely strong dependence of superconductivity on disorder in Sr_2RuO_4," Phys. Rev. Lett. 80, 161 (1998).

37. T. M. Riseman, P. G. Kealey, E. M. Forgan, A. P. Mackenzie, L. M. Galvin, A.W. Tyler, S. L. Lee, C. Ager, D. Mck. Paul, C. M. Aegerter, R. Cubitt, Z-Q. Mao, T. Akima, and Y. Maeno, "Observation of a square flux-line lattice in the unconventional superconductor Sr_2RuO_4," Nature 396, 242 (1998).

38. F. Laube, G. Goll, H. v. Lohneysen, M. Fogelstrom, and F. Lechtenberg, "Spin-triplet superconductivity in Sr_2RuO_4 probed by Andreev reflection," Phys. Rev. Lett. 84, 1595 (2000).

39. Z. Q. Mao, K. D. Nelson, R. Jin, Y. Liu, and Y. Maeno, "Observation of Andreev surface bound state of the 3-K phase in Sr_2RuO_4," Phys. Rev. Lett. 87, 037003 (2001).

40. K. Ishida, H. Mukuda, Y. Kitaoka, K. Asayama, Z. Q. Mao, Y. Mori, Y. Maeno, "Spin-triplet superconductivity in Sr_2RuO_4 identified by ^{17}O Knight shift," Nature 396, 658 (1998).

41. J. A. Duffy, S. M. Hayden, Y. Maeno, Z. Mao, J. Kulda, and G. J. McIntyre, "Polarized-neutron scattering study of the Cooper-pair moment in Sr_2RuO_4," Phys. Rev. Lett. 25, 5412 (2000).

42. H. Murakawa, K. Ishida, K. Kitagawa, Z.Q. Mao, and Y. Maeno, "Measurement of the ^{101}Ru-Knight shift of superconducting Sr_2RuO_4 in a parallel magnetic field," Phys. Rev. Lett. 93, 167004 (2004).

43. H. Murakawa, K. Ishida, K. Kitagawa, H. Ikeda, Z. Q. Mao, and Y. Maeno, " ^{101}Ru Knight Shift Measurement of Superconducting Sr_2RuO_4 under small magnetic fields parallel to the RuO_2 plane," J. Phys. Soc. Japan 76, 024716 (2007).

44. R. Jin, Y. Liu, Z. Mao, and Y. Maeno, "Selection rule in Josephson coupling Between a conventional *s*-wave superconductor and Sr_2RuO_4," Europhys. Lett. 51, 341 (2000).

45. K. D. Nelson, Z. Q. Mao, Y. Maeno, and Y. Liu, "Odd-parity superconductivity in Sr_2RuO_4," Science 306, 1151-1154 (2004).

46. G. M. Luke, Y. Fudamoto, K. M. Kojima, M.I. Larkin, J. Merrin, B. Nachumi, Y.J. Uemura, Y. Maeno, Z. Q. Mao, Y. Mori, H. Nakamura, and M. Sigrist, "Time-reversal-symmetry-breaking superconductivity in Sr_2RuO_4," Nature 394, 558 (1998).

47. J. Xia, Y. Maeno, P. T. Beyersdorf, M. M. Fejer, and A. Kapitulnik, "High resolution polar Kerr effect measurements of Sr_2RuO_4: Evidence for broken time-reversal symmetry in the superconducting state," Phys. Rev. Lett. 97, 167002 (2006).

48. F. Kidwingira, J.D. Van Harlingen, and Y. Maeno, "Dynamical superconducting order parameter domains in Sr_2RuO_4," Science 314, 1267 (2006).

49. J. R. Kirtley, C. Kallin, C. W. Hicks, E.-A. Kim, Y. Liu, K. A. Moler, Y. Maeno, and K. D. Nelson, "Upper limit on supercurrents in Sr_2RuO_4,," Phys. Rev. B 76, 014526 (2007).

50. C. W. Hicks, J. R. Kirtley, T. M. Lippman, N. C. Koshnick, M. E. Huber, Y. Maeno, W. M. Yuhasz, M. B. Maple, and K. A. Moler,"Limits on superconductivity-related magnetization in Sr_2RuO_4 and $PrOs_4Sb_{12}$ from scanning SQUID microscopy," Phys. Rev. B 81, 214501 (2010).

51. Y. A. Ying, X. Cai, Z. Wang, Y. Xin, D. Fobes, T. J. Liu, Z. Q. Mao, and Y. Liu, " Phase-sensitive measurements on chiral surface currents in spin-triplet superconductor Sr_2RuO_4," to be submitted (2015).

52. M. Matsumoto and M. Sigrist, "Quasiparticle States near the surface and the domain wall in a $p_x \pm ip_y$-wave superconductor," J. Phys. Soc. Japan 68, 994 (1999).

53. J. A. Sauls, Z. Zou, and P. W. Anderson, "Josephson tunneling between superconductors with different spin and space symmetries," unpublished (1985).

54. V. B. Geshkenbein and A.I. Larkin, "The Josephson effect in superconductors with heavy fermions," JETP Lett. 43, 395 (1986).

55. A. Millis, D. Rainer, and J.A. Sauls, "Quasiclassical theory of superconductivity near magnetically active interfaces," Phys. Rev. B 38, 4504 (1988).

56. S-K. Yip, "Weak link between conventional and unconventional superconductors," J. Low Temp. Phys. 91, 203 (1993).

57. K. A. Delin and A. W. Kleinsasser, "Stationary properties of high-critical-temperature proximity effect Josephson junctions," *Supercond. Sci Technol.* 9, 227 (1996).

58. V. Ambegaokar and A. Baratoff, "Tunneling between superconductors," *Phys. Rev. Lett.* 10, 486 (1963); *erratum*, 11, 104 (1963).

59. Y. Asano, Y. Tanaka, M. Sigrist, and S. Kashiwaya, "Josephson current in *s*-wave-superconductor/Sr_2RuO_4 junctions," Phys. Rev. B 67, 184505 (2003).

60. D. J. van Harlingen, "Phase sensitive tests of the symmetry of the pairing state in the high-temperature superconductors-Evidence for d_{x2-y2} symmetry," Rev. Mod. Phys. 67, 515 (1995).

61. C. C. Tsuei and J.R. Kirtley, "Pairing symmetry in cuprate superconductors," Rev Mod. Phys. 72, 969 (2000).

62. V. B. Geshkenbein, A. I. Larkin, and A. Barone, "Vortices with Half Magnetic Flux Quanta in Heavy-Fermion Superconductors," Phys. Rev. B 36, 235-238 (1987).

63. A. J. Leggett, "Josephson experiments on the high-temperature superconductors," Phil. Mag. B 74, 509 - 522 (1996).

64. W. Guichard, M. Aprili, O. Bourgeois, T. Kontos, J. Lesueur, and P. Gandit, "Phase sensitive experiments in ferromagnetic-based Josephson junctions," Phys. Rev. Lett. 90, 167001 (2003).

65. M. Tinkham, "Introduction to Superconductivity," 2nd Ed., (McGraw-Hill, Inc.), p226 (1996).

66. D. A. Wollman, D. J. van Harlingen, W. C. Lee, D. M. Ginsberg, and A. J. Leggett, "Experimental determination of the superconducting pairing state in YBCO from the phase coherence of YBCO-Pb dc SQUIDs," Phys. Rev. Lett. 71, 2134 (1993).

67. D. A. Brawner and H. R. Ott, "Evidence for an unconventional superconducting order parameter in $YBa_2Cu_3O_{6.9}$," Phys. Rev. B 50, 6530 (1994).

68. A. Mathai, Y. Gim, R. C. Black, A. Amar, and F. C. Wellstood, "Experimental proof of a time-reversal-invariant order parameter with a π shift in $YBa_2Cu_3O_{7-\delta}$," Phys. Rev. Lett. 74, 4523 (1995).

69. D. A. Wollman, D. J. van Harlingen, J. Giapintzakis, and D. M. Ginsberg, "Evidence for d_{x2-y2} pairing from the magnetic field modulation of $YBa_2Cu_3O_{7-\delta}$/Pb Josephson junctions," Phys. Rev. Lett. 74, 797 (1995).

70. D. A. Brawner and H. R. Ott, "Evidence for a non-*s*-wave superconducting order parameter in $YBa_2Cu_3O_{6.9}$ with T_c = 60 K" Phys. Rev. B 53, 8249 (1996).

71. B. Chesca, R. R. Schulz, B. Goetz, C. W. Schneider, A. Schmehl, H. Bielefeldt, H. Hilgenkamp, J. Mannhart, and C. C. Tsuei, "Design and realization of an all *d*-wave dc π-superconducting quantum interference device," App. Phys. Lett. 912 (2000).

72. R. R. Schulz, B. Chesca, B. Goetz, C.W. Schneider, H. Hilgenkamp, and J. Mannhart, "*d*-wave induced zero-field resonances in dc π-superconducting quantum interference device," Phys. Rev. Lett. 88, 177003 (2002).

73. N. Shirakawa, K. Murata, S. Nishizaki, Y. Maeno, and T. Fujita, "Pressure dependence of superconducting critical temperature of Sr_2RuO_4," *Phys. Rev. B* 56, 7890-7893 (1997).

74. K. Yoshida, F. Nakamura, T. Goko; T. Fujita, Y. Maeno; Y. Mori, and S. NishiZaki, "Electronic crossover in the highly anisotropic normal state of Sr_2RuO_4," *Phys. Rev. B* 58, 15062-15066 (1998).

75. T. Nomura and K. Yamada, "Magnetic properties of quasi-two-dimensional ruthenates studied by mean field theoretical approach," *J. Phys. Soc. Jpn.* 69, 1856-1864 (2000).

76. N. Okuda, T. Suzuki, Z. Mao, Y. Maeno, and T. Fujita, "Unconventional strain dependence of superconductivity in spin-triplet superconductor Sr_2RuO_4," *J. Phys. Soc. Jpn.* 71, 1134-1139 (2002).

77. S. Kittaka, Taniguchi, H., Yonezawa, S., Yaguchi, H. & Maeno, Y. Higher-T_c superconducting phase in Sr_2RuO_4 induced by uniaxial pressure. Phys. Rev. B 81**,** 180510(R) (2010).

78. Y. Maeno, T. Ando, Y. Mori, E. Ohmichi, and S. Ikeda, S. NishiZaki, and S. Nakatsuji, "Enhancement of Superconductivity of Sr_2RuO_4 to 3 K by Embedded Metallic Microdomains," *Phys. Rev. Lett.* 81, 3765-3768 (1998).

79. S. Kittaka, H. Yaguchi, and Y. Maeno, "Large Enhancement of 3-K Phase Superconductivity in the Sr_2RuO_4-Ru Eutectic System by Uniaxial Pressure," *J. Phys. Soc. Jpn.* 78, 103705 (2009).

80. M. Walker and P. Contreras, "Theory of elastic properties of Sr_2RuO_4 at the superconducting transition temperature," *Phys. Rev. B* 66, 214508 (2002).

81. C. W. Hicks, D. O. Brodsky, E. A. Yelland, A. S. Gibbs, J. A. N. Bruin, M. E. Barber, S. D. Edkins, K. Nishimura, S. Yonezawa, Y. Maeno, and A. P. Mackenzie, "Strong increase of T_c of Sr_2RuO_4 under both tensile and compressive strain," *Science* 344, 283-285 (2014).

82. Y. A. Ying, Y. Xin, B. W. Clouser, E. Hao, N. E. Staley, R. J. Myers, L. F. Allard, D. Fobes, T. Liu, Z. Q. Mao, and Y. Liu, "Suppression of proximity effect and the enhancement of *p*-wave superconductivity in the Sr_2RuO_4-Ru system," Phys. Rev. Lett. 103, 247004 (2009).

83. Y. A. Ying, N. E. Staley, Y. Xin, K. Sun, X. Cai, D. Fobes, T. J. Liu, Z. Q. Mao, and Y. Liu, "Dislocations and the enhancement of superconductivity in odd-parity superconductor Sr_2RuO_4," Nature Communications 4, Article number: 2596 doi:10.1038/ncomms3596 (2013).

84. T. L. Hughes, H. Yao, and X-L. Qi, "Majorana zero modes in dislocations of Sr_2RuO_4," Phys. Rev. B 90, 235123 (2014)

85. A. I. Larkin, Z. Eksp, *Fiz. Pis'ma Red. 2, 205* (1965).

86. A. Millis, S. Sachdev, and C. Varma, "Inelastic scattering and pair breaking in anisotropic and isotropic superconductors," *Phys. Rev. B* 37, 4975-4986 (1988).

87. R. Radtke, K. Levin, H. B. Schüttler and M. Norman, "Predictions for impurity-induced T_c suppression in the high-temperature superconductors," *Phys. Rev. B* 48, 653-656 (1993).

88. Z. Mao, Y. Mori, and Y. Maeno, "Suppression of superconductivity in Sr_2RuO_4 caused by defects," *Phys. Rev. B* 60, 610-614 (1999).

89. N. Kikugawa, A. Mackenzie, C. Bergemann, R. Borzi, S. Grigera, and Y. Maeno, "Rigid-band shift of the Fermi level in the strongly correlated metal: $Sr_{2-y}La_yRuO_4$," *Phys. Rev. B* 70, 060508 (2004).

90. N. Kikugawa and Y. Maeno, "Non-Fermi-liquid behavior in Sr_2RuO_4 with nonmagnetic impurities," *Phys. Rev. Lett* 89, 117001 (2002).

91. N. Kikugawa, A. P. Mackenzie, and Y. Maeno, "Effects of in-plane impurity substitution in Sr_2RuO_4," *J. Phys. Soc. Jpn.* 72, 237-240 (2003).

92. Z. Q. Mao, Y. Maenoab, and H. Fukazawa, "Crystal growth of Sr_2RuO_4". *Materials Research Bulletin* 35, 1813-1824 (2000).

93. I. A. Firmo, S. Lederer, C. Lupien, A. P. Mackenzie, J. C. Davis, and S. A. Kivelson, "Evidence from tunneling spectroscopy for a quasi-one-dimensional origin of superconductivity in Sr_2RuO_4," Phys. Rev. B 88, 134521 (2013).

94. S. Madhavan, D. G. Schlom, A. Dabkowski, H. A. Dabkowska, and Y. Liu, "Growth of epitaxial *a*-axis and *c*-axis oriented Sr_2RuO_4 films," App. Phys. Lett. 68, 559 (1996).

95. M. A. Zurbuchen, Y. Jia, S. Knapp, A.H. Carim, D.G. Schlom, L-N. Zou, and Y. Liu, "Suppression of superconductivity by crystallographic defects in epitaxial Sr_2RuO_4 films," Appl. Phys. Lett. 78, 2351-2353 (2001).

96. L. Miao, W. Zhang, P. Silwal, X, Zhou, I. Stern, T. Liu, J. Peng, J. Hu, D. H. Kim, and Z. Q. Mao, "Epitaxial strain effect on transport properties in $Ca_{2-x}Sr_xRuO_4$ thin films," Phys. Rev. B 88, 115102 (2013).

97. Y. Krockenberger, M. Uchida, K. S. Takahashi, M. Nakamura, M. Kawasaki, and Y. Tokura, "Growth of superconducting Sr_2RuO_4 thin films," Appl. Phys. Lett. 97, 082502 (2010).

98. M. Sigrist and H. Monien, "Phenomenological theory of the 3 Kelvin phase in Sr_2RuO_4," J. Phys. Soc. Japan 70, 2409 (2001).

99. Z. Q. Mao, K.D. Nelson, R. Jin, Y. Liu, and Y. Maeno, "Observation of Andreev surface bound state of the 3-K phase in Sr_2RuO_4," Phys. Rev. Lett. 87, 037003 (2001).

100. L. J. Buchholtz and G. Zwicknagl, "Identification of *p*-wave superconductors," Phys. Rev. B 23, 5788 (1981).

101. C-R. Hu, "Midgap surface states as a novel signature for $d_{x^2-y^2}$-wave superconductivity," Phys. Rev. Lett. 72, 1526 (1994).

102. Y. Tanaka and S. Kashiwaya, "Theory of tunneling spectroscopy of *d*-wave superconductors," Phys. Rev. Lett. 74, 3451 (1995).

103. K. Sengupta, H-J. Kwon, and V. M. Yakovenko, "Edge states and determination of pairing symmetry in superconducting Sr_2RuO_4," Phys. Rev. 65, 104504 (2002).

104. D. A. Ivanov, "Non-Abelian statistics of half-quantum vortices in *p*-wave superconductors," Phys. Rev. Lett. 86, 268 (2001).

105. S. Das Sarma, C. Nayak, and S. Tewari, "Proposal to stablize and detect half-quantum vortices in strontiun ruthenate thin films: Non-Abelian braiding statistics of vortices in $p_x + p_y$ superconductors," Phys. Rev B 73, 220502(R) (2006).

106. S. Das Sarma, M. Freedman, and C. Nayak, "Topologically protected qubits from a possible non-Abelian fractional quantum Hall state," Phys. Rev. Lett. 94, 166802 (2005).

107. J. Jang, D. G. Ferguson, V. Vakaryuk, R. Budakian, S. B. Chung, P. M. Goldbart, and Y. Maeno, "Observation of Half-Height Magnetization Steps in Sr_2RuO_4," Science 331, 186 (2011).

108. X. Cai, Y. A. Ying, N. E. Staley, Y. Xin , D. Fobes, T. Liu , Z. Q. Mao, and Y. Liu, "Quantum oscillations in small rings of odd-parity superconductor Sr_2RuO_4," Phys. Rev. B 87, 081104(R) (2013).

109. K. Miyake and O. Narikiyo, "Model for unconventional superconductivity of Sr_2RuO_4: Effect of impurity scattering on time reversal breaking triplet pairing with a tiny gap," Phys. Rev. Lett. 83, 1423 (1999).

110. Y. Hasegawa, K. Machida, and M. Ozaki, "Spin-triplet superconductivity with line nodes in Sr_2RuO_4," J. Phys. Soc. Jpn. 69, 336 (2000).

111. M. J. Graf and A.V. Balatsky, "Identifying the pairing symmetry in the Sr_2RuO_4 superconductor," Phys. Rev. B 62, 9697 (2000).

112. H. Won and K. Maki, "Possible f-wave superconductivity in Sr_2RuO_4?" Europhys. Lett. 52, 427-433 (2000).

113. M. E. Zhitomirsky and T.M. Rice, "Interband proximity effect and nodes of superconducting gap in Sr_2RuO_4," Phys. Rev. Lett. 87, 057001 (2001).

114. D.F. Agterberg, T.M. Rice, and M. Sigrist, "Orbital dependent superconductivity in Sr_2RuO_4," Phys. Rev. Lett. 78, 3374 (1997).

115. P. Monthoux and G.G. Lonzarich, "*p*-wave and *d*-wave superconductivity in quasi-two-dimensional metals," Phys. Rev. B 59, 14598 (1999).

116. T. Kuwabara and M. Ogata, "Spin-triplet superconductivity due to antiferromagnetic spin-fluctuation in Sr_2RuO_4," Phys. Rev. Lett. 85, 4586 (2000).

117. K. K. Ng and M. Sigrist, "The role of spin-orbit coupling for the superconducting state in Sr_2RuO_4," Europhys. Lett. 47, 473 (2000).